communications biology

A Nature Portfolio journal

Article

https://doi.org/10.1038/s42003-025-08386-0

Identification of potent inhibitors of *Leishmania donovani* and *Leishmania infantum chagasi*, the causative agents of Old and New World visceral leishmaniasis

Bilal Zulfiqar[1,2], Fabio Antonio Colombo[3], Juliana Barbosa Nunes[4], Patricia Ferreira Espuri[5], Aurea Favero Ferreira[4], Sujatha Manthri[6], Manu De Rycker[6], Marcos Jose Marques[5] & Vicky M. Avery[1,2]

The drug discovery pipeline for neglected kinetoplastid diseases remains sparse. In particular, the field of leishmaniasis drug discovery has had limited success in translating potential drug candidates into viable therapies. Here, we describe the development of two lead compounds, **BZ-1** and **BZ1-I**, which have potent in vitro anti-leishmanial activity against *Leishmania donovani* DD8 intracellular amastigotes (0.59 ± 0.13 μM and 0.40 ± 0.38 μM) with corresponding selectivity (> 33.89 and > 49.12) for differentiated THP-1 cells (Human monocytic cell line), respectively. Further characterization and biological profiling identified that in addition to the activity against *L. donovani* DD8 (Old World - Indian strain), compounds were active against intracellular parasites from other species and strains of the Old and New World, namely *L. donovani* (Old World - Sudanese strain) and *L. infantum chagasi* (New World-South American strain). In vivo evaluation using the hamster model illustrated that the activity observed in vitro was translated in vivo, with outstanding results. Our data suggests that these compounds represent a promising starting point for developing a novel lead series for future anti-leishmanial therapeutics.

Kinetoplastid parasites of the genus *Leishmania* are the causative agent of the infectious disease, leishmaniasis[1], endemic in 98 countries, with more than one billion people at risk of acquiring the disease[2,3]. The mode of transmission is via the bite of a sand fly, genus *Phlebotomus* (Old World) and *Lutzomyia* (New World)[4]. The life cycle of the *Leishmania* parasite exists between the sand fly (promastigote form) and the mammalian host (amastigote form)[5]. Current treatment regimens often have poor toxicity profiles and resistance has begun to emerge against the standard of care therapies[6,7]. There also exists a significant imbalance in the drug discovery pipeline for leishmaniasis[8,9], with ongoing challenges including insufficient understanding of the pathogen biology, plus a lack of cellular and pathophysiological animal models that mimic the disease in humans[10–12]. An additional hurdle for new chemical entities is the variation in activity often observed against different species, contributing to different clinical outcomes based on geographical location of the parasite[13–16]. Many compounds in the past have exhibited efficacy against *Leishmania* species, including antibiotics, organo-metallics, nucleosides and sterol biosynthesis inhibitors[17–20]. Most of these were not progressed due to host cell cytotoxicity, plus lack of efficacy and safety in in vivo models. Even the currently available treatments face similar issues. Pentavalent antimonials, the treatment of choice in South America, Africa, Nepal, Bangladesh, and India (except North Bihar)[21], have demonstrated differences in in vitro sensitivity between the different species in the amastigote macrophage models. *L. brasiliensis* and *L. donovani* were shown to be three to five fold more sensitive to antimonials compared to *L. tropica*, *L. major* and *L. mexicana*[22,23]. Amphotericin B deoxycholate is considered the second-line therapy in cases

[1]Discovery Biology, Centre for Cellular Phenomics, Griffith University, Nathan, Queensland, 4111, Australia. [2]School of Environment and Science, Griffith University, Nathan, Queensland, 4111, Australia. [3]Department of Clinical and Toxicological Analysis, Faculty of Pharmaceutical Sciences, Federal University of Alfenas, Minas Gerais, Brazil. [4]Department of Pathology, University of São Paulo, São Paulo, Brazil. [5]Department of Pathology and Parasitology, Institute of Biomedical Sciences, Federal University of Alfenas, Minas Gerais, Brazil. [6]Drug Discovery Unit, University of Dundee, Dundee, United Kingdom.
e-mail: v.avery@griffith.edu.au

that do not respond to antimonials[24] as it was very effective against visceral leishmaniasis (>90% cure rate)[25]. A study conducted by Escobar et al. compared the sensitivity of different *Leishmania* species to amphotericin B, observing that the rank order of species sensitivities measured in Median effective dose (ED_{50}), was *L. mexicana* > *L. aethiopica* > *L. tropica* > *L. major* > *L. panamensis* > *L. donovani* for the promastigote assay and *L. mexicana* > *L. panamensis* > *L. aethiopica* > *L. tropica* > *L. major* > *L. donovani* for the amastigote assay"[26]. Variations in drug sensitivities of different species have also been demonstrated in vitro for miltefosine with *L. tropica*, *L. aethiopica*, *L. mexicana*, *L. panamensis* and *L. donovani*[27]. The Half maximal effective concentration (EC_{50}) values obtained for miltefosine varied from 2.63 to 10.63 μM between these species, whereas the EC_{50} for *L. major* was found to be significantly lower at 37.17 μM[26]. Paromomycin has been approved by World Health Organization (WHO) for the treatment of cutaneous leishmaniasis in its topical form[28]. In vitro testing suggests that sensitivity to paromomycin in *Leishmania* amastigotes in murine macrophages varies between species. This drug tends to be more effective against *L. tropica* and *L. major* compared to *L. mexicana* and *L. braziliensis* when compared in the same assay models[19]; and is moderately active against all strains of *L. donovani* (mean IC_{50} in-between 6.1 and 43.8 μM), except *L. donovani* DD8 (mean IC_{50} 158.1–165.7 μM)[19]. The basis for this difference has not yet been elucidated.

A target candidate profile (TCP) and a target product profile (TPP) were developed by Drugs for Neglected Diseases Initiative (DND*i*) for visceral leishmaniasis to guide the progression of compounds in the drug discovery pipeline[29]. These guidelines define the minimum criteria for developing a safe, effective, and orally administered anti-leishmanial drug that can be used in a short treatment regimen, aiming to replace current therapies[29].

As per the DND*i* TCP, for a compound to be considered an active hit against visceral leishmaniasis, the molecule should exhibit activity against the intracellular amastigote stage of *L. donovani* or *L. infantum* with an IC_{50} value below 10 μM. The compound must show at least a 10-fold selectivity over mammalian cell lines. Additionally, it should not possess any structural alerts that could negatively affect its metabolism, stability, or reactivity and demonstrate no toxicity in both in silico and in vivo models[29].

Historically, drug discovery for leishmaniasis has been slow and inefficient, primarily due to the limited commitment of the pharmaceutical industry for neglected tropical diseases (NTDs). Collectively, the lack of financial incentive, as well as the complexity of *Leishmania* biology, has resulted in few novel drugs entering the pipeline in recent decades. Nevertheless, recent advancements in drug discovery and greater engagement from pharmaceutical and philanthropic partners have begun to reshape this landscape, offering hope for more effective treatments[16,30]

This study involved screening a structurally diverse synthetic library in an effort to discover new compounds active against *Leishmania donovani* (MHOM/IN/80/DD8). Hit molecules were defined as active against both promastigote and intracellular amastigote stages, with minimal cytotoxicity not only against the host cell THP-1 (human monocytic cell), but also a panel of mammalian cells comprised of various cell lines from human and mice representing different organ systems including HepG2 (human liver cancer cell), HEK-293 (human embryonic kidney cell), RAW 264.7 and J774.1 (both murine macrophages) cell lines. This panel served as a valuable tool to address compound cytotoxicity early in development. Two 1H-cyclopenta[b]quinolin-9-amine compounds (**BZ1** and **BZ1-I**) that fulfilled the hit criteria with respect to both activity and selectivity were subjected to further in vitro and in vivo profiling.

To compare the difference of activity between the Old world and New world species, two species of *Leishmania* were selected, namely *L. donovani* causing visceral leishmaniasis in the Indian subcontinent WHO reference strain MHOM/IN/80/DD8 (Old world)[31] and *L. infantum chagasi* (New world) which causes visceral leishmaniasis in Brazil, MHOM/BR/1972/BH46[32]. In addition, to compare the strain specific differences, *L. donovani* MHOM/SD/62/1S-CL2D, LdBOB-eGFP (Old world)[33], a genetically modified strain of a wild type isolated from the Sudanese population was also utilized. Histopathological and cytokine data were acquired to determine whether the compounds elicited an immunological response against the *Leishmania* infection.

Results

Discovery of compound BZ1

Compound N-(4-Ethoxyphenyl)-2,3-dihydro-1H-cyclopenta[b]quinolin-9-amine, referred to herein as **BZ1** (Fig. 1A) was discovered via a screening campaign. From 5560 compounds tested in the promastigote assay, 29 compounds fulfilled our criteria having >60% activity at 10 μM (hit rate:

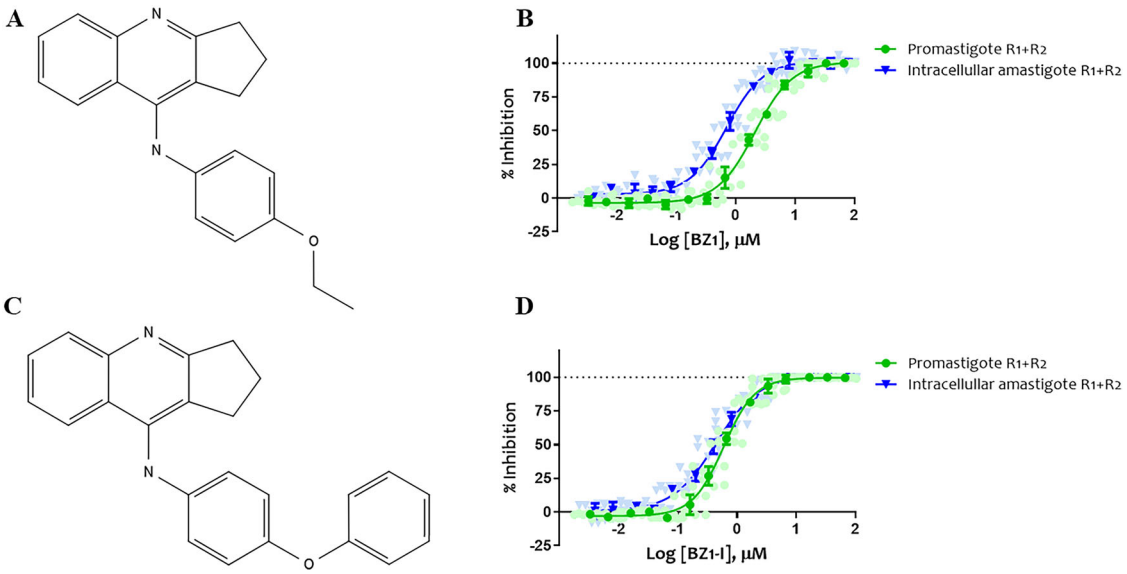

Fig. 1 | Structures and in vitro activities of compound BZ1 and BZ1-I. A Structure of compound "N-(4-Ethoxyphenyl)-2,3-dihydro-1H-cyclopenta[b]quinolin-9-amine" referred as BZ1. **B** In vitro activity of the compound BZ1 against *L. donovani* DD8 intracellular amastigote promastigotes. **C** Structure of compound "N-(4-phenoxyphenyl)-1H,2H,3H-cyclopenta[b]quinolin-9-amine" referred to as BZ1-I. **D** In vitro activity of the compound BZ1-I against *L. donovani* DD8 intracellular amastigotes and promastigotes. The data points are means and error bars represent standard deviations of three replicates of two independent experiments. Individual data points are shown as lighter-shaded markers in the corresponding colour of each group.

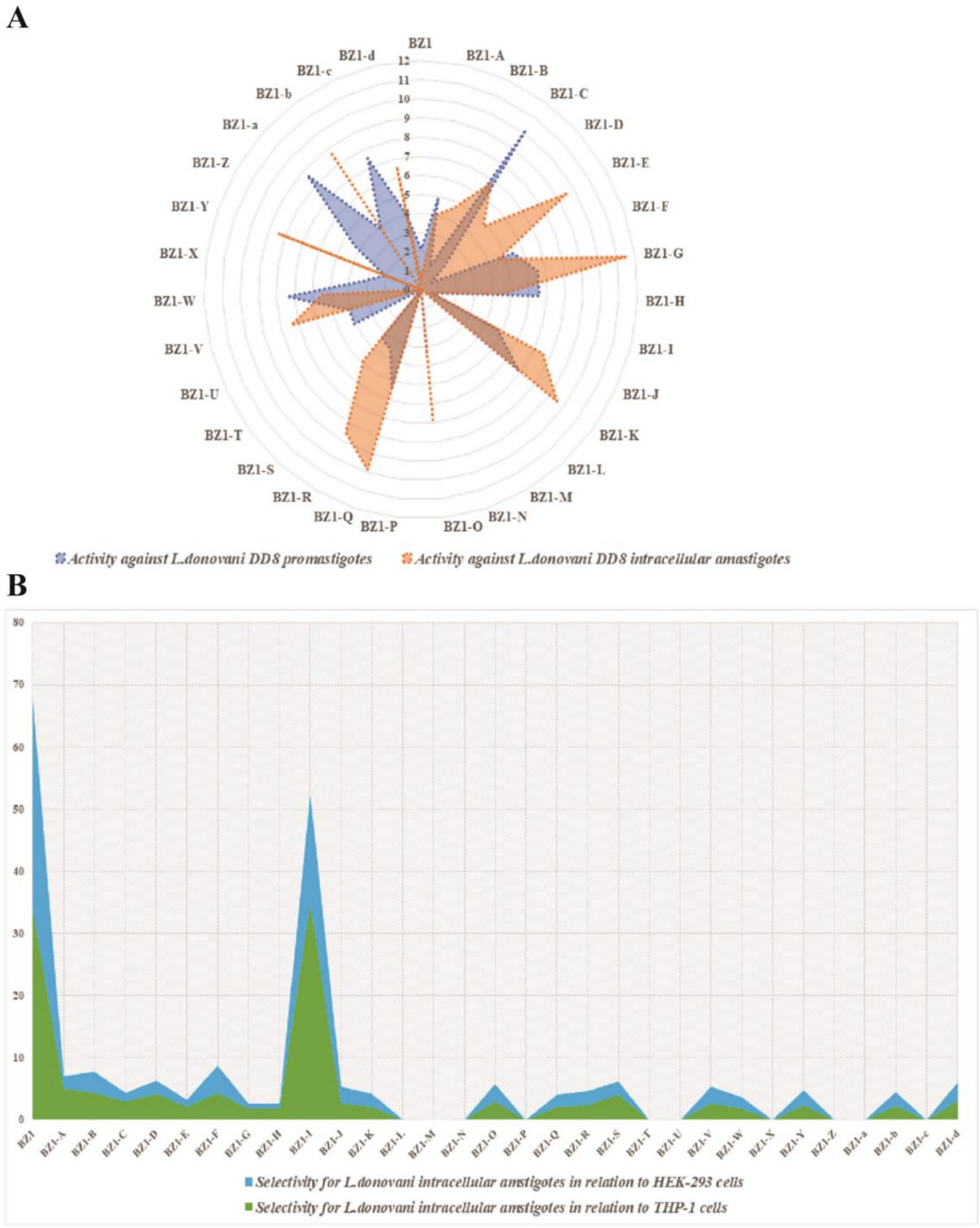

Fig. 2 | Anti-parasitic activity exhibited by analogues against both *Leishmania* promastigotes and intracellular amastigotes, with associated selectivity for HEK-293 and THP-1 host cells. A Spider plot of the IC_{50} values of compounds for *L. donovani* DD8 promastigotes (blue) and *L. donovani* DD8 intracellular amastigotes (orange). **B** Selectivity of compounds active against *L. donovani* intracellular amastigotes in relation to HEK-293 (blue) and THP-1 cells (green).

0.52%). Of these, 22 compounds returned activity at >60% activity against the promastigotes when retested at 10 μM. Testing against the intracellular amastigote identified 40 compounds with >50% activity at 10 μM, which was the criteria defined for a hit molecule, and representing a hit rate of 0.71%. Following retest, 26 of these compounds reconfirmed activity at 10 μM.

Of the compounds which confirmed upon retest, four demonstrated >50% activity against both the promastigote and the amastigote forms at

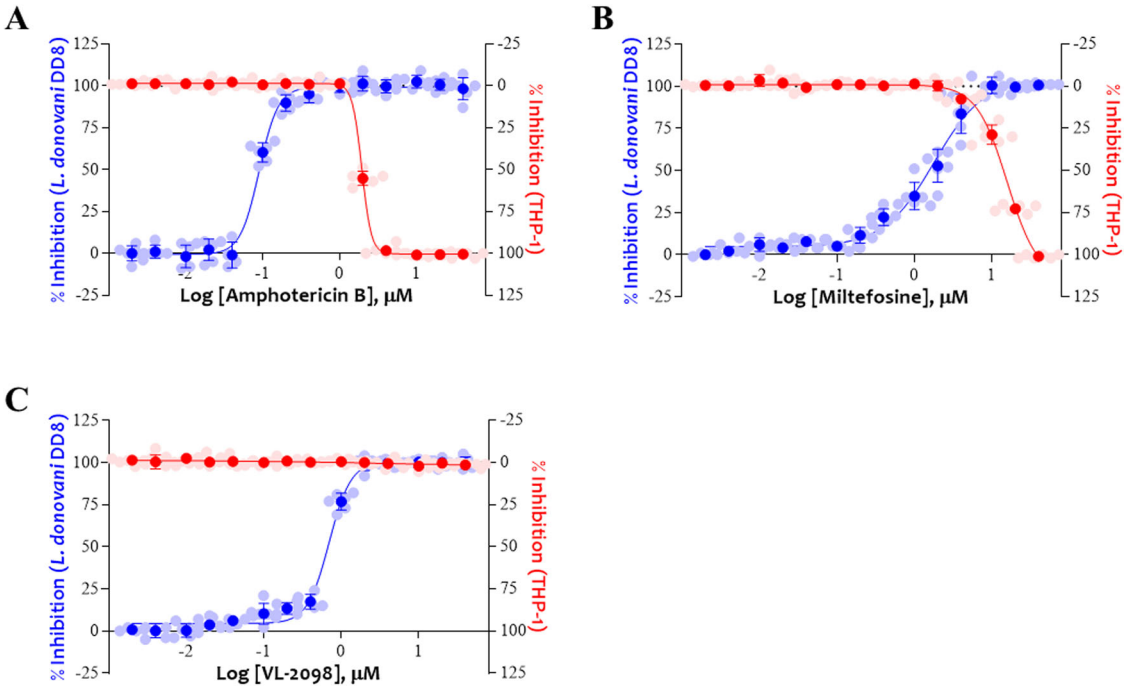

Fig. 3 | In vitro activity of the reference drugs against *L. donovani* DD8 intracellular amastigotes. **A** Amphotericin B, **B** miltefosine and **C** VL-2098. The percentage inhibition was determined from quadruplicate assay data points after normalization of the data with 1 µM amphotericin B (100% death, final assay) as the positive control and 0.4% DMSO (0% inhibition) as the negative control. Left-*Y*-axis: percentage inhibition of *L. donovani* DD8 (blue dots/triangles and curves); Right-*Y*-axis: percentage inhibition of THP-1 cells (red dots/triangles and curves); *X*-axis: Log of micromolar compounds concentration. Data points are means and error bars represent the standard deviations of two independent experiments (dots for experiment 1 and triangles for experiment 2). Individual data points are represented as lighter-shaded markers in the corresponding colour of each group.

10 µM. The most promising hit molecule **BZ1** had an IC_{50} value of 0.59 ± 0.13 µM against the intracellular amastigotes and an IC_{50} value of 2.37 ± 0.85 µM against the extracellular promastigotes (Fig. 1B). The selectivity index of **BZ1** was estimated to be >33 for both HEK-293 and THP-1 cells.

A series of substructure searches, performed in Scifinder® (CAS, American Chemical Society), ChemSpider® (Royal Society of Chemistry) and ChEMBL® (European Bioinformatics Institute), in addition to Compounds Australia® structural portal (CASPeR) were performed to retrieve analogues most relevant to structure–activity relationship (SAR) interpretation. Analogues with no structural alerts (metabolism/stability/reactivity) were chosen based on the following criteria: no more than 5 H-bond donors (total number of N–H and O–H bonds), no more than 10 H-bond acceptors (all N or O atoms), and a molecular mass < 500 g/mol and octanol–water partition coefficient (log *P*) < 5. Thirty compounds were selected (referred to as **BZ1-A**–**BZ1-d**), the structures of which are shown in Supplementary Fig. 1.

Of the 30 analogues tested against *L. donovani* DD8 promastigotes and amastigotes, compound **BZ1-I** (Fig. 1C), showed improved activity (IC_{50}: 0.60 ± 0.04 µM) against the promastigotes compared to the original hit compound, **BZ1** (IC_{50}: 2.15 ± 0.14 µM). **BZ1-I** also demonstrated comparable activity (IC_{50}: 0.40 ± 0.38 µM) to **BZ1** against the intracellular form of the parasite (amastigotes)(IC_{50}: 0.59 ± 0.13 µM) (Fig. 1D).

The activity exhibited by these analogues against both the *Leishmania* promastigotes and intracellular amastigotes has been presented in the form of a spider plot (Fig. 2A). Selectivity of these compounds for the *Leishmania* intracellular amastigotes, with respect to HEK-293 and THP-1 host cells, is shown in Fig. 2B. According to the target candidate profile (TCP) established by DND*i*, we aimed to identify compounds with an IC_{50} value < 10 µM against *L. donovani* intracellular amastigotes and 10-fold more selective for the parasites than mammalian cells. The DND*i* guidelines provide the minimal requirements for the development of a safe, oral, effective anti-leishmanial drug, enabling short course treatment schedule with a bid to replace the existing current treatments available.

The IC_{50} values of the reference drugs, amphotericin B, miltefosine and the preclinical candidate, VL-2098, were determined for the intracellular amastigote assay; amphotericin B 0.08 ± 0.01 µM (Fig. 3A), miltefosine 1.97 ± 0.25 µM (Fig. 3B) and VL-2098 0.70 ± 0.13 µM (Fig. 3C). The negative control, 0.4% DMSO, was used to define 100% viability of the amastigotes in the host cells. Amphotericin B was used at 1 µM as the positive control, to define 0% viability of amastigotes in the host cells and no associated host cell cytotoxicity.

Activity on different strains and species of *Leishmania* in the Old and New World

The intracellular amastigote activities of **BZ1** and **BZ1-I** were compared between the different strains and species of *Leishmania* representative of Old and New World leishmaniasis (Table 1). It was observed that our novel compounds, **BZ1** and **BZ1-I**, demonstrated sub-micromolar activity against *L. donovani* WHO reference strain MHOM/IN/80/DD8 which results in visceral leishmaniasis in the Indian subcontinent[34], with IC_{50} values of 0.59 ± 0.13 and 0.40 ± 0.38 µM, respectively, in the intracellular amastigote assay (Fig. 4A, B). In contrast, the IC_{50} values of both **BZ1** and **BZ1-I** were found to be 4.40 ± 0.12 and 4.26 ± 0.24 µM against *L. donovani* MHOM/SD/62/1S-CL2D, LdBOB-eGFP intracellular amastigotes, a genetically modified strain, the wild type of which was isolated from the Sudanese population. *L. donovani* MHOM/SD/62/1S-CL2D, LdBOB-eGFP was chosen as it had previously been used for high-content screening[35]. Relative to the variation in activity against the parasite strains, the selectivity for THP-1 cells shifted from >25.64 to >11.76 for **BZ1** and from >44.44 to >11.49 for **BZ1-1**, respectively (Table 1—72 h incubation data). Amphotericin B was used as a reference compound exhibiting IC_{50} values of 0.20 ± 0.02 µM for *L. donovani* MHOM/IN/80/DD8. The reported IC_{50}

Table 1 | Tabulated form of in vitro activity of the BZ1 and BZ1-I against different Old and New World strains and species of *Leishmania* intracellular amastigotes with different incubation times

Compounds and reference drugs	*Leishmania donovani* (MHOM/IN/80/DD8)			*Leishmania donovani* (MHOM/IN/80/DD8)			*Leishmania donovani* (MHOM/SD/62/1S-CL2D, LdBOB)		
Incubation period with compounds	96 h incubation			72 h incubation					
	IC_{50} (μM) [mean ± SD]	Selectivity		IC_{50} (μM) [mean ± SD]	Selectivity		IC_{50} (μM) [mean ± SD]	Selectivity	
		HEK-293 cells	THP-1 cells		HEK-293 cells	THP-1 cells			THP-1 cells
BZ1	0.59 ± 0.13	>33.72	>33.89	0.78 ± 0.27	>25.51	>25.64	4.40 ± 0.12		>11.76
BZ1-I	0.40 ± 0.38	>24.11	>49.12	0.45 ± 0.28	>44.22	>44.44	4.26 ± 0.24		>11.49
Amphotericin B	0.20 ± 0.02	47.61	10.24	0.60 ± 0.18	19.38	4.16	–		–
Miltefosine	2.54 ± 0.57	15.66	>7.87	3.78 ± 0.73	10.52	>5.29	–		–

values for miltefosine were 2.54 ± 0.57 μM for *L. donovani* MHOM/IN/80/DD8.

In the cytotoxicity assay, a stable plateau of activity was not observed for either **BZ1** or **BZ1-I** at 80 μM (final assay concentration) which was the highest concentration tested due to compound solubility issues in 100% DMSO, hence accurate IC_{50} values could not be determined (Fig. 4C, D). Arbitrary IC_{50} values were therefore calculated for compounds against HepG2, Raw264.7, J774.1, HEK-293 and THP-1 cells (Supplementary Table 1).

The promastigote activities of **BZ1** and **BZ1-I** were compared between the different strains and species of Leishmania representative of Old and New World leishmaniasis (Table 2).

Determining cidal action of compounds (Promastigote assay)

Compound activity can either be cidal (direct killing) or static in nature, thus has the ability to hinder parasite division, resulting in a delayed response. The time and concentration dependent susceptibility of the BZ compounds was evaluated in comparison to known reference compounds/drugs. Measurement of the number of promastigotes following exposure to the compounds at various concentrations for 24, 48 and 72 h are shown in Fig. 5. To determine cidal activity, physical deformation and loss of motility allowed accurate assessment of live/dead parasite. No viable promastigotes were observed for amphotericin B, miltefosine, **BZ1** and **BZ1-I** at 0.33, 6.66, 6.66, and 1.66 μM respectively after 24 h incubation (Fig. 5A), indicating that at these concentrations, the mode of action of these compounds was direct killing.

Time to kill assay (promastigotes and intracellular amastigote assay)

Ascertaining the "time to kill" can serve as a determinant of anti-leishmanial compound activity relative to the time needed to kill the parasite, ideally as fast as possible. To determine the speed with, which the compounds exerted their effects, the IC_{50} values of **BZ1** and **BZ1-I** were determined for both promastigotes and amastigotes. **BZ1** activity against promastigotes showed a plateau of activity from 24 h (4.31 ± 0.22 μM) onwards (considered as 2 concentrations or more at >90%), suggesting that **BZ1** was able to achieve 100% inhibition of the parasite number reduction after 24 h (Fig. 5B). After 48 h the IC_{50} value of **BZ1** was consistent (2.37 ± 0.74 μM) remaining in the same range for 96 h. In contrast, whilst **BZ1-I** also demonstrated 100% kill at 24 h (3.08 ± 1.11 μM) there was a significant shift in IC_{50} value at 48 h (0.69 ± 0.35 μM) (Fig. 5C) which then stabilized. This suggested **BZ1-I** was a faster acting compound than **BZ1** against the promastigotes at 48 h time point. For the intracellular amastigote assay **BZ1** did not elicit a stable plateau of activity (100% inhibition) until after 48 h incubation time (Fig. 5D). **BZ1-I** demonstrated activity within 24 h (4.84 ± 0.83 μM) however with significantly reduced efficacy than observed for the longer incubation periods (0.40 ± 0.38 μM) (Fig. 5E). Stable consistent activity was observed after 48 h. This delay in **BZ1** and **BZ1-I** complete activity, or suboptimal effects, might be due to permeability issues, as the compounds must cross multiple barriers to reach the amastigotes which reside within the parasitophorous vacuoles. Alternatively, this may also reflect the nature of the mode of action of this compound, highlighting an accumulative effect following increased incubation times. Overall, this would warrant future investigations as we believe this is an interesting finding.

Generating resistant cell lines

Resistance was generated for both **BZ1** and **BZ1-I**. In parallel, resistance was also generated for the reference drugs amphotericin B and miltefosine to enable assessment of **BZ1** and **BZ1-I** against amphotericin B and miltefosine resistant parasites, thus informing whether the compounds acted via a similar mechanism of action to these drugs. After a duration of 428 days, clones of resistant strains were generated for amphotericin B (Fig. 6A), miltefosine (Fig. 6B) and **BZ1** (Fig. 6C) that could withstand concentrations of these drugs/compounds of 420 nM, 40 and 11 μM, respectively. Resistant clones were also generated for **BZ1-I** taking 210 days to reach a

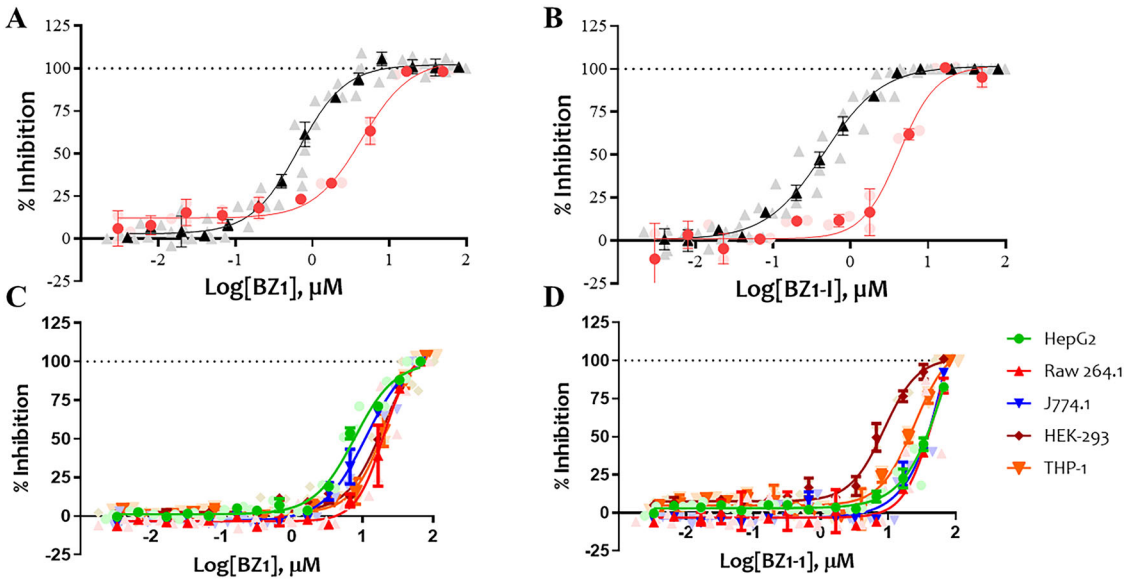

Fig. 4 | In vitro activity and selectivity of the BZ1 and BZ1-I compounds against different species and strains causing VL. A Concentration response curve (CRC) of the in vitro activity of the compound **BZ1** generated against *L. donovani* DD8 and *L. donovani* LdBOB intracellular amastigotes for 72 h incubation time. **B** Concentration response curve of the In vitro activity of the compound **BZ1-I** generated against *L. donovani* DD8 and *L. donovani* LdBOB intracellular amastigotes. For **A** and **B**, Black line represents *L. donovani* DD8 and Red for *L. donovani* LdBOB. **C** In vitro cytotoxicity represented as CRC for compound **BZ1** against a panel of mammalian cell lines for 72 h incubation time. **D** In vitro cytotoxicity represented as CRC of the compound **BZ1-1** against a panel of mammalian cell lines for 72 h incubation time. For both figure **C** and **D** the green line represents HepG2 cells, red line represents Raw 264.1, blue line represents J774.1 cells, burgundy line represents HEK-293 cells and orange line represents THP-1 cells. For the activity against the *L. donovani* LdBOB (**A**, **B**), the data represents the mean and standard devitaion of three independent replicates (each replicate run as a single technical replicate). For **C**, **D** the data represents the mean and standard deviations of three replicates of two independent experiment ($N = 2$). Individual data points are indicated as lighter-shaded markers in the corresponding colour of each group.

concentration of 5.5 µM, (Fig. 6D). Continued exposure to increase resistance to **BZ1-I** is ongoing. When both compounds were compared, resistance generated with **BZ1-I** occurred more rapidly than **BZ1**, suggesting a different mechanism or uptake.

Resistance in these clonal populations for amphotericin B (Fig. 6E), miltefosine (Fig. 6F), **BZ1** (Fig. 6G) and **BZ1-I** (Fig. 6H) were confirmed using both promastigote and intracellular amastigote assays. The results obtained co-align with previously reported data for amphotericin B and miltefosine, where a 14-fold increase in drug resistance was obtained for miltefosine[36] and a 20-fold resistance generated for amphotericin B[37].

Studies were also conducted to determine the stability of resistance after removing drug pressure for 10 passages for amphotericin B (Fig. 6I), miltefosine (Fig. 6J), **BZ1** (Fig. 6K) and **BZ1-I** (Fig. 6L). Compounds **BZ1** and **BZ1-I** resulted in IC_{50} values of 5.35 ± 0.18, 4.94 ± 0.69, 14.52 ± 0.55, and 8.93 ± 0.67 µM for the intracellular amastigote and promastigote assays, respectively. The IC_{50} values obtained were compared with a control non-resistant culture of the same passage number. Our results indicated that resistance was stable for all reference and test compounds after removal of drug pressure.

Following the confirmation of resistance generation and stability, the activity of **BZ1** and **BZ1-I** was evaluated on *L. donovani* DD8 strains resistant to amphotericin B and miltefosine, using the promastigote and intracellular amastigote assays, respectively. The findings reveal no significant difference in the activity of **BZ1** and **BZ1-I** against the resistant strains compared to the wild-type *L. donovani* DD8 strain (Fig. 7). These results suggest that both compounds exert their antiparasitic effects through a mechanism distinct from that of amphotericin B and miltefosine.

Drug metabolism and pharmacokinetics studies

Effective anti-leishmanial drugs must exhibit favorable properties to ensure bioavailability, target specificity, and minimal off-target effects. Both compounds were analyzed for parameters critical to oral drug absorption and pharmacokinetic performance. The summary and interpretation of key metrics has been outlined in Tables 3 and 4.

In vivo efficacy

To fully appreciate the potential of **BZ1** and **BZ1-I** for visceral leishmaniasis, the compounds were assessed in a chronic hamster model allowing parasite load evaluation in two target organs (liver and spleen), as for the human disease. The in vivo efficacy of **BZ1** and **BZ1-I** against *L. infantum chagasi* (MHOM/BR/1972/BH46), was assessed in the *L. infantum chagasi* chronic phase hamster model (Fig. 8A). Post 60 days infection the animals were administered with 0.5% of carboxymethyl cellulose (vehicle) suspension orally ($n = 5$ animals), (untreated vehicle only group, or UTG); 50 mg/kg/day of GLU (Meglumine Antimoniate), by intraperitoneal injection (GLU group; $n = 5$); 10 mg/kg/day of **BZ1** or **BZ1-I**, administered orally as suspensions in 0.5% of carboxymethyl cellulose ($n = 6$ each group) for 10 consecutive days, with repeated doses each day. Meglumine antimoniate is a pentavalent antimony (SbV) drug, used with a maximum dose of 20 mg/kg intramuscularly to treat all types of leishmaniasis and is recommended as the first line treatment option by WHO[38,39]. Upon completion of the experiment, animals were sacrificed in a carbon dioxide (CO_2) chamber, and a sample of the spleen and the liver (~50 mg) removed, weighed, and used for total RNA extraction. Real-time PCR quantification of the amastigotes per gram was determined post treatment in spleen and liver samples to ascertain efficacy. The standard curve for DNA for *L. infantum chagasi* (MHOM/BR/1972/BH46) promastigotes presented optimal linearity and reproducibility (Fig. 8B), with $R^2 = 0.9925$, indicating a high correlation between the variables. Cycle thresholds (Ct) linearity describes the degree to which the cycle thresholds for the parasite number is precisely proportional to the promastigotes in the spleen and liver samples. The detection limit of the curve corresponds to Ct of 41.52. The Ct values obtained from the spleen and liver samples were inserted into the equation of the line and the number of parasites calculated per gram of organ.

Table 2 | Tabulated form of in vitro activity of the BZ1 and BZ1-I against different Old and New World strains and species of *Leishmania* promastigotes

Compounds and Reference drugs	*Leishmania donovani* (MHOM/IN/80/DD8)		*Leishmania infantum chagasi* (MHOM/BR/72/BH46)		*Leishmania amazonensis* (MHOM/BR/71973/M2269)	
	IC_{50} (μM) [mean ± SD]	Selectivity [HEK-293] cells	IC_{50} (μM) [mean ± SD]	Selectivity [Murine peritoneal macrophages]	IC_{50} (μM) [mean ± SD]	Selectivity [murine peritoneal macrophages]
BZ1	2.15 ± 0.14	>9.20	0.64 ± 0.06	>11.95	1.43 ± 0.28	>5.37
BZ1-I	0.60 ± 0.04	>16.01	0.53 ± 0.07	>11.26	1.09 ± 0.25	>5.54
Amphotericin B	0.12 ± 0.01	68.27	1.49 ± 2.21		0.28 ± 0.07	

As shown in Fig. 8C, the average number of parasites in the UTG, was 1.54×10^6/g and 2.09×10^5/g of tissue, in the spleen and liver, respectively, confirming an established infection in these animals (clinical symptoms such as ascites and alopecia). The GLU-treated group resulted in a parasite load reduction, with average values of 1.22×10^4 (spleen) and 2.53×10^3 (liver) reported. Treatment with **BZ1** significantly reduced the number of amastigotes in the spleen to 2.54×10^4/g and liver to 3.02×10^3 when compared with the UTG ($p < 0.005$). These values were comparable to those obtained with GLU. Treatment with **BZ1-I** also reduced the number of amastigotes in the spleen and liver considerably, resulting in 1.62×10^2/g and 1.20×10^2/g respectively, when compared with the group UTG ($p < 0.005$); resulting in ~21-fold greater activity compared to the GLU treatment group.

Histopathological analysis of golden Hamster tissue fragments

Histopathological analysis of the spleen and liver was carried out blinded for all experimental groups with respect to immuno-inflammatory patterns associated with infection by *L. chagasi* (Fig. 9).

Histopathological changes observed in the livers of untreated animals were characterized by the presence of intense mononuclear inflammatory infiltrate in the portal space with the formation of nodules. Of note, intense inflammatory infiltrates of lymphocytes and macrophages forming nodules were observed in the hepatic parenchyma, in addition to evident Kupffer cells hyperplasia and hypertrophy. In the spleen, there was slight hyperplasia of lymphoid follicles in the white pulp and considerable increase of macrophages forming nodules in the red pulp.

The presence of inflammatory nodules in the hepatic parenchyma, lymph histiocytic inflammatory infiltrate in the portal space forming nodules of infected animals treated with **BZ1** was observed in $n = 6$ mice, where **BZ1** was administered orally as suspensions in 0.5% of carboxymethyl cellulose. An increase of macrophages in the red pulp forming nodular aggregates and granulomas was shown in the spleen. Infected animals treated with **BZ1-I** ($n = 6$) showed a mild inflammatory infiltrate in the portal space and nodules in the parenchyma with the presence of giant cells. In the spleen, an evident increase in macrophages in the red pulp with the formation of nodules was observed, in addition to white pulp hypoplasia.

Effect of BZ1 and BZ1-I on cytokine profile

Next, we analyzed the cytokine profile of liver and spleen cells isolated from the in vivo hamster animal model, which we classified as healthy (uninfected), untreated (UTG); treated with GLU; or treated with **BZ1** or **BZ1-I** (Fig. 10). Alterations in both the proinflammatory cytokine INF-γ (Fig. 10A), TNF-α (Fig. 10B) and IL-17 (Fig. 10C) and anti-inflammatory cytokine IL-4 (Fig. 10D), IL-10 (Fig. 10E) and TGF-β (Fig. 10F) profiles representing both the Th1 and Th2 immune responses, were compared between the different groups. As expected, there was a significant difference in INF-γ levels between the untreated and GLU treatment for spleen samples. Compound **BZ1** produced similar results as GLU treatment for the INF-γ levels. A significant downregulation of IL-17 was observed for **BZ1** ($P < 0.001$) compared to GLU in liver samples. A significant downregulation of TNF-α ($P < 0.01$) was observed with **BZ1** treatment compared to GLU and untreated liver and spleen samples. The anti-inflammatory cytokines, such as IL-4 and TGF-β, were also significantly downregulated following exposure to **BZ1** ($P < 0.01$) compared to untreated spleen and liver samples.

Discussion

Much advancement has been made in VL treatment over the last 15–20 years, with the discovery of antimonial monotherapy and the development of newer treatments, such as liposomal formulations of amphotericin B, injectable paramomycin and the first orally available drug miltefosine[16,40]. Nevertheless, these drugs still bear limitations such as poor safety profiles and the need for cold chain storage[41]. Not to mention the associated non-compliance to therapy because of the difficult route of administration and long durations of therapy[30,42]. This calls for an innovative new therapy that is efficacious, safe, has pan-geographical efficacy against multiple species and

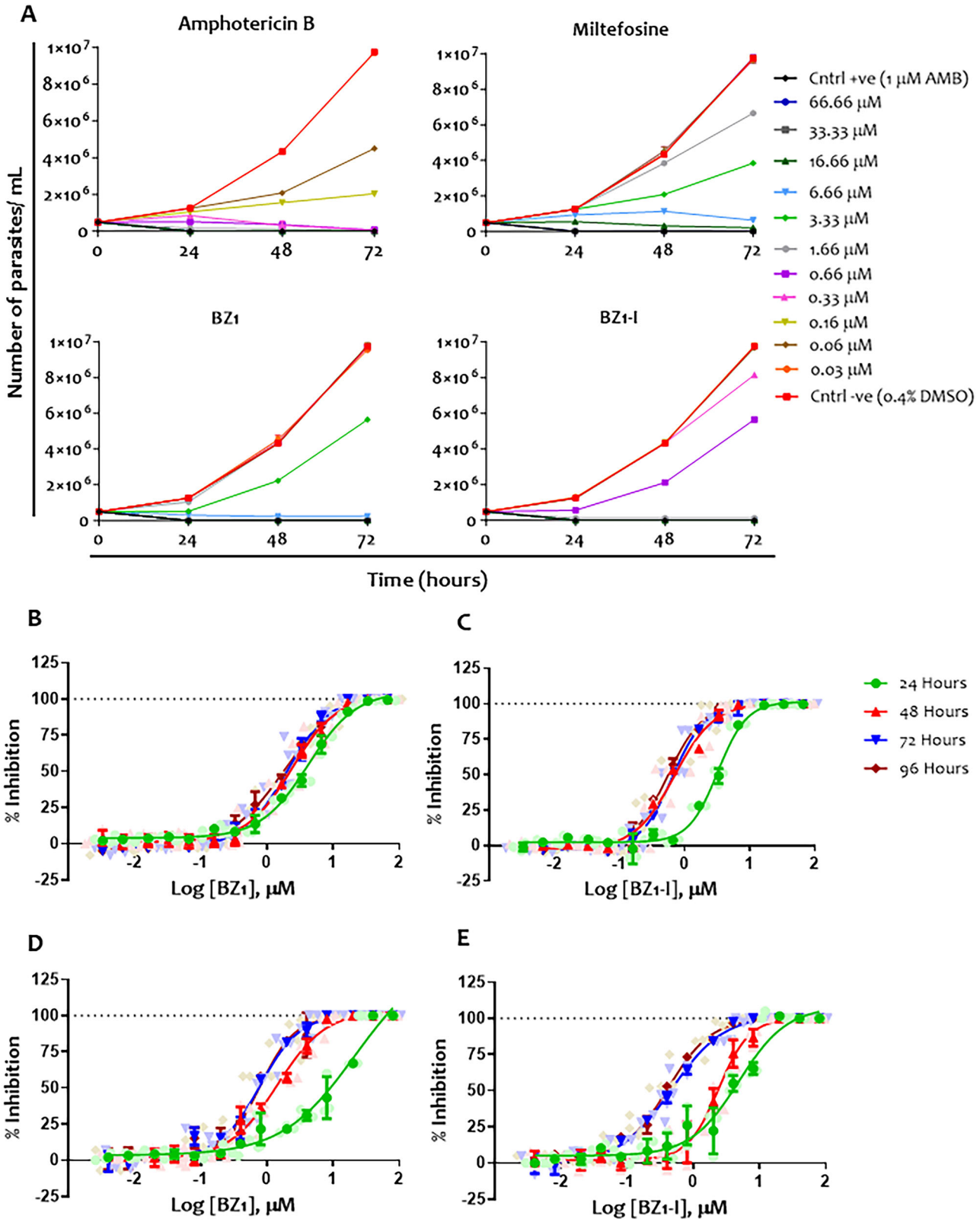

Fig. 5 | Cidal/static mode of action and impact of time on efficacy of compounds BZ1 and BZ1-I. A Cidal activity of amphotericin B, miltefosine, **BZ1** and **BZ1-I** based on MIC at various time intervals 24, 48 and 72 h. Different concentrations are colour-coded ranging 66.66–0.03 µM as described in the figure legend. Each evaluation was performed in triplicate, for $N = 2$. **B** Concentration response curve for **BZ1** against *L. donovani* DD8 promastigote following exposure from 24 to 96 h to ascertain speed of action. **C** Concentration response curve for **BZ1-I**against *L. donovani* DD8 promastigote following exposure from 24 to 96 h to ascertain speed of action. **D** Concentration response curve for **BZ1** against *L. donovani* DD8 intracellular amastigotes following exposure from 24 to 96 h to ascertain speed of action. **E** Concentration response curve for **BZ1-I** against *L. donovani* DD8 intracellular amastigotes following exposure from 24 to 96 h to ascertain speed of action. **B**–**E** Green represents 24 h, red 48 h, blue 72 h and brown 96 h incubation times. Each evaluation was performed in triplicate, for $N = 2$. Individual data points are indicated as lighter-shaded markers in the corresponding colour of each group.

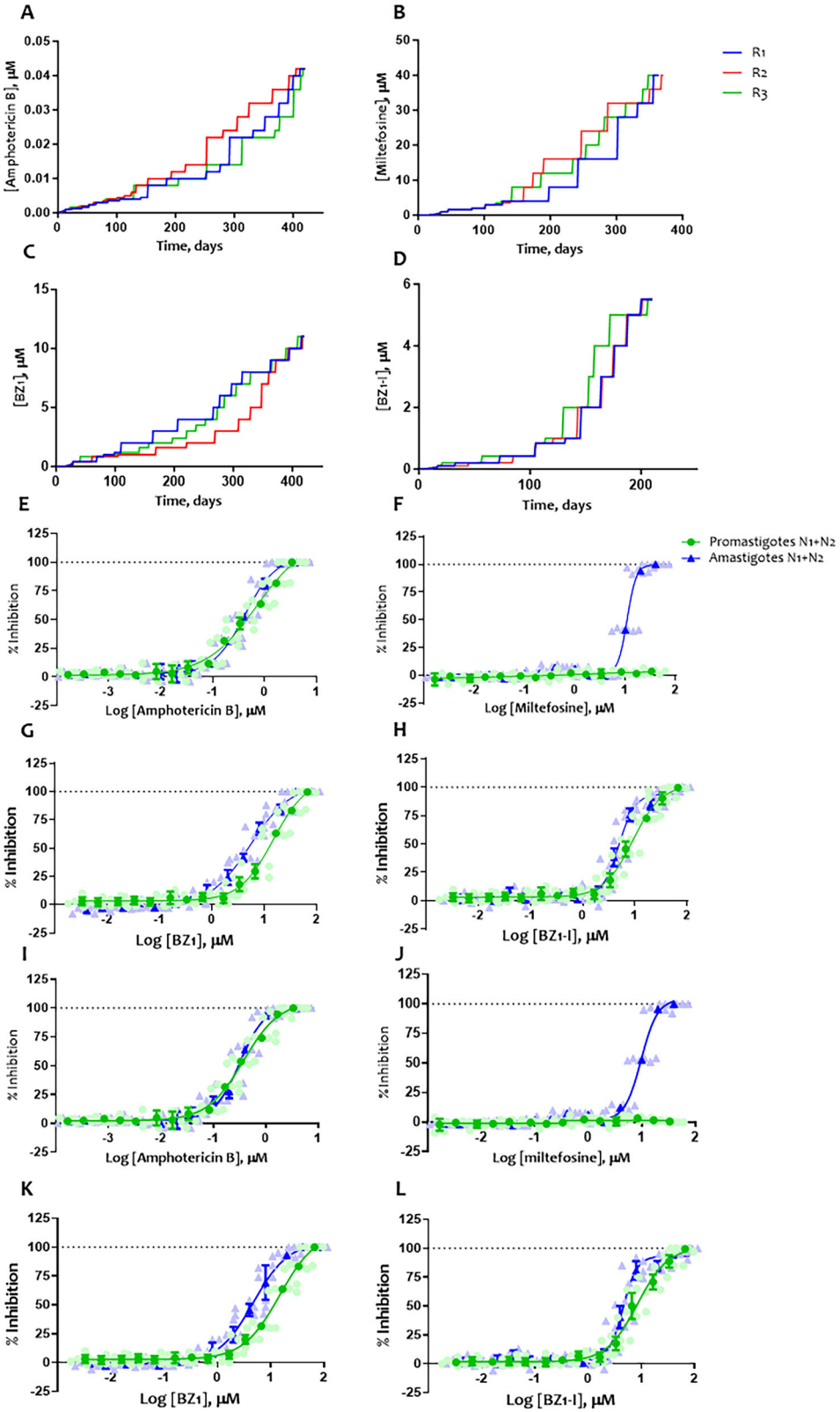

Fig. 6 | Generation of resistance, confirmation and stability of resistance after freeze–thaw cycle in *L. donovani* DD8 promastigotes for both compounds BZ1 and BZ1-I. A Generating resistance against amphotericin B. **B** Generating resistance against miltefosine. **C** Generating resistance against **BZ1**. **D** Generating resistance against **BZ1-I**, line 1 (blue), line 2 (red) and line 3 (green) are representative of 3 different clones. **E** Resistance confirmation against amphotericin B after freeze–thaw cycle in promastigote and intracellular amastigote assays. **F** Resistance confirmation against miltefosine after freeze–thaw cycle in promastigote and intracellular amastigote assays. **G** Resistance confirmation against **BZ1**after freeze–thaw cycle in promastigote and intracellular amastigote assays. **H** Resistance confirmation against **BZ1-I**after freeze–thaw cycle in promastigote and intracellular amastigote assays. **I** Resistance stability against amphotericin B after freeze–thaw cycle in promastigote and intracellular amastigote assays. **J** Resistance stability against miltefosine after freeze–thaw cycle in promastigote and intracellular amastigote assays. **K** Resistance stability against **BZ1** after freeze–thaw cycle in promastigote and intracellular amastigote assays. **L** Resistance stability against **BZ1-I** after freeze–thaw cycle in promastigote and intracellular amastigote assays. Green and red represent promastigote assay N1 and N2, respectively. Blue and brown represent intracellular amastigote assay N1 and N2, respectively. Each evaluation was performed as duplicates for $N = 2$. Individual data points are represented as lighter-shaded markers in the corresponding colour of each group.

strains responsible for the disease. Here we report the discovery of two compounds from phenotypic screening and the subsequent data that supports their selection for further development as candidates for VL.

Compound **BZ1** (N-(4-Ethoxyphenyl)-2,3-dihydro-1H-cyclopenta[b]quinolin-9-amine), exhibited activity against both the intracellular (amastigote) and extracellular (promastigote) forms of the *Leishmania donovani* DD8 (Old World- Indian strain) parasite, with IC_{50} values 0.59 ± 0.13 and 2.37 ± 0.85 µM, respectively. **BZ1** also displayed good selectivity (>33) for the mammalian host cells THP-1 and an independent cell line, HEK-293 cells. Thus, **BZ1** fulfilled the Drugs for Neglected diseases initiative (DND*i*) target candidate profile criteria for promising molecules based on this in vitro activity and selectivity profile[29]. It also does not have

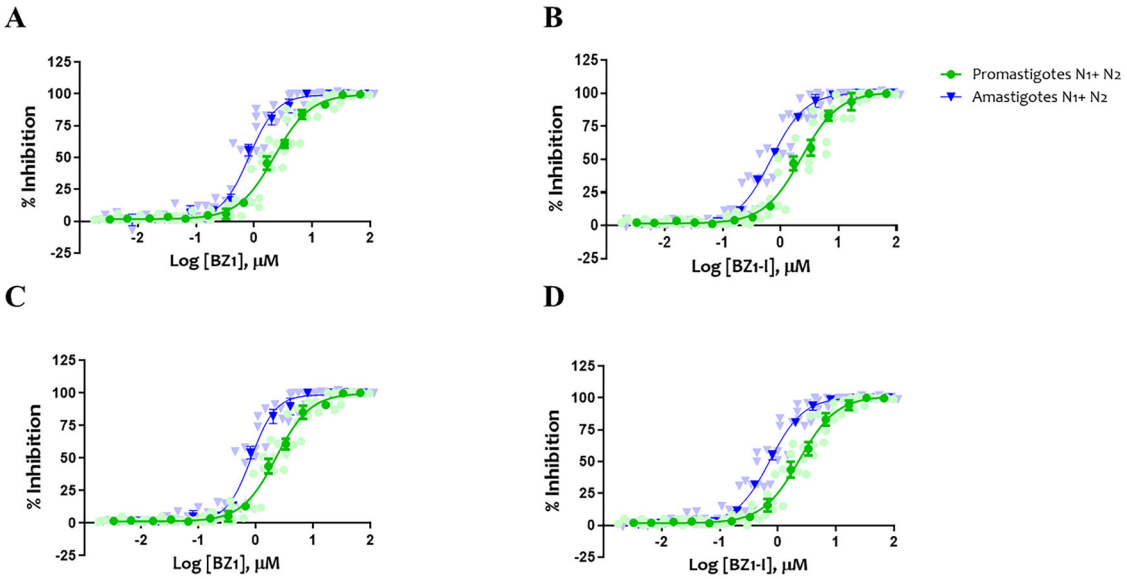

Fig. 7 | In vitro activity of compounds BZ1 and BZ1-I on the amphotericin B and miltefosine resistant parasites utilizing the promastigote and the intracellular amastigote assays. A In vitro activity of compounds **BZ1** on amphotericin B resistant parasites. **B** In vitro activity of compounds **BZ1-I** on amphotericin B resistant parasites. **C** In vitro activity of compounds **BZ1** on miltefosine resistant parasites. **D** In vitro activity of compounds **BZ1-I**on miltefosine-resistant parasites. Each evaluation was performed as duplicates for $N = 2$. Individual data points are shown as lighter-shaded markers in the corresponding colour of each group.

Table 3 | Physiochemical properties of compounds BZ1 and BZ1-I

Parameter	BZ1	BZ1-I	Remarks
Molecular weight (MW)	304.39	352.44	Both compounds fall within the optimal MW range (<500 Da) for oral bioavailability.
Polar surface area (PSA) (Å²)	35.4	35.4	Low PSA indicated favourable permeability across biological membranes.
Fraction rotatable bonds (FRB)	4	4	Moderate flexibility; suitable for drug-likeness.
Hydrogen bond donors (HBD)	1	1	Low HBD enhances membrane permeability.
Hydrogen bond acceptors (HBA)	3	2	Fewer HBAs supported lipophilicity and target binding.
Aromatic rings	3	4	Multiple aromatic rings may aid in target binding via π–π interactions.
Fsp^3	0.25	0.13	Low Fsp^3 may reduce solubility but increase target specificity.
Predicted pK_a	Basic: 8.1	Basic: 8.1	Basicity may influence interactions with the acidic environments in the parasitic lifecycle.
*c*Log*P*	4.7	6.0	**BZ1-I** is more lipophilic, potentially enhanced passive permeability but risking poor solubility.
*c*Log*D* at pH 7.4	3.9	5.2	Higher cLogD of **BZ1-I** indicated stronger nonspecific binding to plasma proteins.
*g*Log*D* at pH 7.4	5.0	>5.3	Excessive lipophilicity of **BZ1-I** could impair pharmacokinetics and lead to aggregation.
Solubility (Sol 2.0/6.5 µg/mL)	>100/12.5–25	25–50/1.6–3.1	**BZ1** showed superior solubility compared to **BZ1-I**, especially at pH 6.5, relevant to parasitic environments.

Table 4 | The pharmacokinetic properties of the compounds BZ1 and BZ1-I, based on human microsome studies, revealing their metabolic stability and clearance potential

Parameter	BZ1	BZ1-I	Remarks
T1/2 (min)	47	57	Both compounds exhibited moderate metabolic stability.
CLint, in vitro (µL/min/mg protein)	37	31	Comparable in vitro clearance rates, indicating manageable metabolism.
Predicted CLint, in vivo (mL/min/kg)	30	25	**BZ1-I** showed slightly lower intrinsic clearance, favouring longer half-life.
Predicted CLblood (mL/min/kg)	12	11	Both compounds demonstrated moderate blood clearance, enhancing systemic exposure.
Predicted extraction ratio (EH)	0.59	0.55	Moderate EH values align with intermediate clearance classifications.
Clearance classification	Intermediate	Intermediate	Suitable for further optimization but not optimal for high-clearance pathways.

any structural alerts and does not exhibit in vivo toxicity in the hamster VL model.

Liposomal amphotericin B (LAMB) is the treatment of choice in the Indian subcontinent and Mediterranean regions[43,44]. Whilst both amphotericin B deoxycholate (Fungizone®) and liposomal amphotericin (LAMB) (Ambisome®) have shown potent activity[45] against the different species of *Leishmania*, both variants have significant adverse effects including nephrotoxicity, thrombophlebitis and hypokalemia[46]. When compared with amphotericin B, which has an IC_{50} 0.20 ± 0.02 µM in the *L. donovani* DD8 intracellular amastigote assay (96 h), **BZ1** had ~3 fold lower in vitro activity

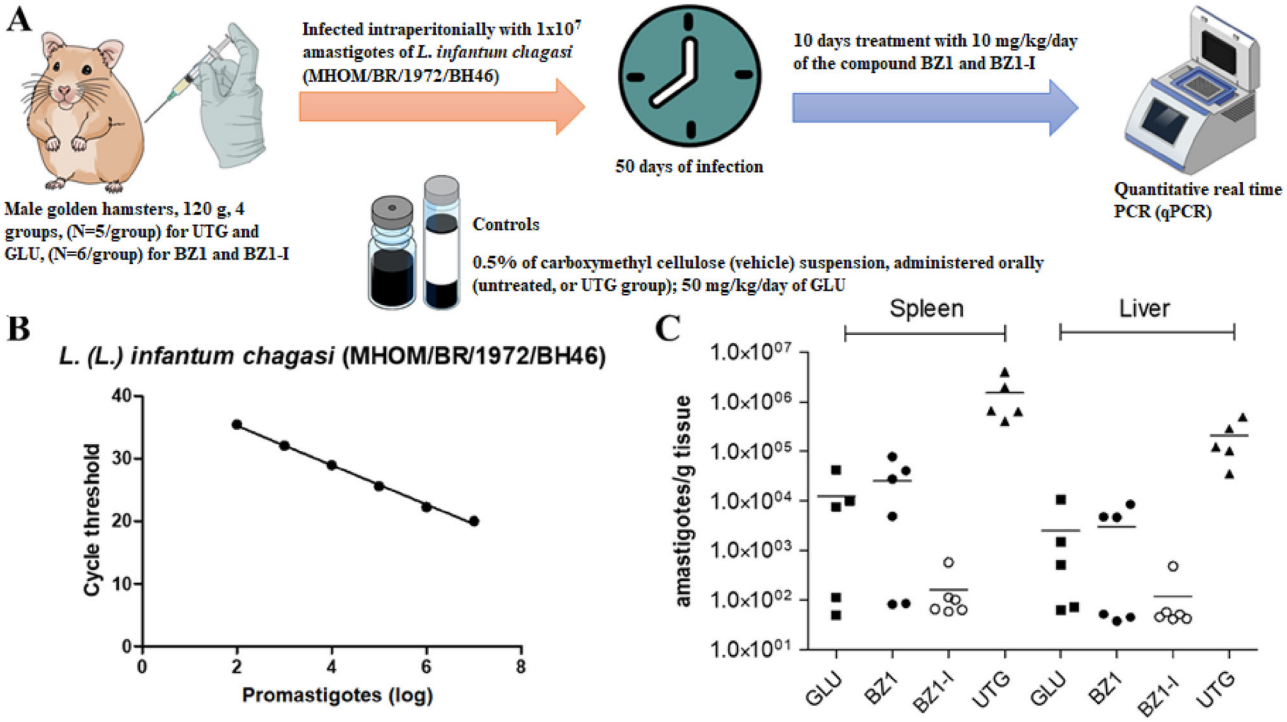

Fig. 8 | In vivo activity of compounds BZ-1 and BZ1-I in the L. infantum chagasi hamster model. A Schematics of in vivo *L. infantum chagasi* (MHOM/BR/1972/BH46) Hamster model. **B** Standard curve for serial dilutions of DNA from promastigote forms from *L. infantum chagasi* (MHOM/BR/1972/BH46) culture to determine the absolute number of parasites present per gram of sample. **C** Real-time PCR quantification (amastigotes per gram in spleen and liver) to measure the in vivo efficacy of **BZ1** and **BZ1-I** in the *L. infantum chagasi* (MHOM/BR/1972/BH46) Hamster model. GLU: meglumine antimoniate, UTG: untreated control.

(0.59 ± 0.13 μM) in the same assay. However, **BZ1** had a greater selectivity index (SI) for the THP-1 host cells, with >33 compared to amphotericin B which is 10.24.

In comparison to the other reference drug, miltefosine, which is also used in combination with LAMB in the clinical settings[47], displayed an IC_{50} of 2.54 ± 0.57 μM in the *L. donovani* DD8 intracellular amastigote assay (96 h), whereas **BZ1** demonstrated 5-fold greater activity (0.59 ± 0.13 μM) in the same assay. **BZ1** also demonstrated an improved selectivity profile (>33) than miltefosine, as the SI of miltefosine is only 15.66 and 7.87 for HEK-293 and THP-1 cells, respectively. Overall, **BZ1** showed better in vitro selectivity profiles than the currently used drugs available.

Initial SAR studies, with the objective of illustrating biological proof of concept for this chemical class, included thirty compounds (**BZ1-A–BZ1-d**), resulting in a range of IC_{50} values from 0.57 to 11.48 μM for the intracellular amastigote assay (Supplementary Table 2). Analogue **BZ1-I** demonstrated improved activity against the *L. donovani* DD8 intracellular amastigotes (IC_{50} 0.40 ± 0.38 μM) and comparable activity to **BZ1** against *L. donovani* DD8 intracellular amastigotes (IC_{50} 0.59 ± 0.13 μM). The SI for **BZ1-I** was >49.12 and >24.11 for THP-1 host cells and HEK-293, respectively, when compared to the activity observed against the intracellular amastigote.

Our goal was to establish a strong foundation of efficacy and supportive pharmacological profile, to ascertain the therapeutic potential of the candidates, subsequently enabling more informed and targeted medicinal chemistry efforts.

Whilst in vitro anti-leishmanial activity has been reported for chemotypes from the class of Quinolines and 9-Anilinoacridines[48–50], of which the BZ compounds are members, there are no previous reports of **BZ1** and **BZ1-I** anti-leishmanial activity.

It has been reported that therapeutic efficacy is dependent on the species of *Leishmania*, geographic region and clinical manifestations, therefore experimental and clinical data should not be generalized[23,30,51]. The taxonomic classification for the genus *Leishmania* is based on the molecular and biochemical characterization of each species[1]. These differences contribute to the variable sensitivity of compounds and may present important clinical implications[52,53]. It has been reported in the past that a three to five-fold intrinsic variation in drug sensitivity exists among *Leishmania* species for antimonials, azoles, miltefosine and paromomycin[14,23,27].

A variation in activity was observed for compounds **BZ1** and **BZ1-I** following the pattern of increased activity from *L. donovani* (MHOM/IN/80/DD8) > *L. donovani* (MHOM/SD/62/1S-CL2D, LdBOB). To minimize the possibility of methodology impacting the data[16], all evaluations were undertaken using the same image-based approach[54].

The data suggested that the variation of the in vitro activity between the strains is substantial. This is most evident in the case of *L. donovani* (MHOM/IN/80/DD8) and *L. donovani* (MHOM/SD/62/1S-CL2D, LdBOB), with a 5-fold and 10-fold difference in activity for **BZ1** and **BZ1-I** in the intracellular amastigote 72 h assay, respectively. Possible reasons for the difference in in vitro activity between the two strains exist, such as media components used in the assay (media composition, fetal bovine serum); multiplicity of infection and biological make-up of the parasites themselves or the specific target of the molecule.

The physicochemical parameters (Table 3) of a compound significantly influence its bioavailability, permeability, and ability to interact with the target pathogen, whereas the pharmacokinetic properties (Table 4) of these compounds, reveal their metabolic stability and clearance potential. Both compounds show promising drug-likeness, with **BZ1** exhibiting a better solubility and balanced lipophilicity, which are critical for achieving adequate systemic concentrations and minimizing off-target effects. On the other hand, **BZ1-I**, with higher lipophilicity, risks aggregation and lower solubility but may have stronger permeability.

Leishmaniasis is characterized by the parasite's need for intracellular survival, making permeability, solubility, and metabolic stability critical for a compound's effectiveness. We believe **BZ1** is the more promising candidate for anti-leishmanial drug discovery due to its favorable solubility, balanced lipophilicity, and sufficient metabolic stability. Whereas **BZ1-I** requires

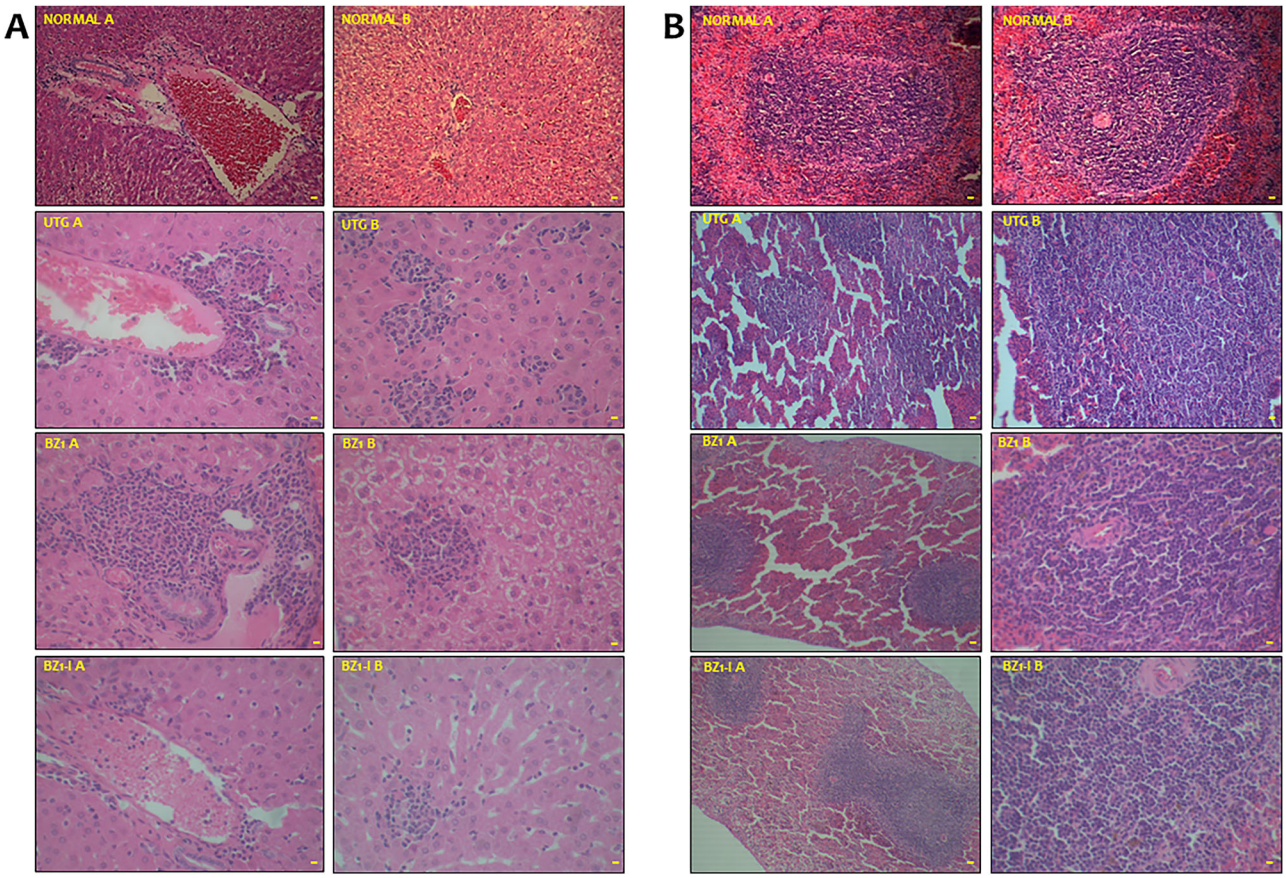

Fig. 9 | Histopathological analysis of golden Hamster tissue fragments. **A** Fragments of liver processed histologically and stained with Haematoxylin and Eosin in *L. infantum chagasi* (MHOM/BR/1972/BH46) hamster model. **B** Fragments of spleen processed histologically and stained with Haematoxylin and Eosin in *L. infantum chagasi* (MHOM/BR/1972/BH46) Hamster model. Normal: Healthy control, UTG: Untreated control. The scale bar (20 μm) is shown as a yellow line.

optimization to reduce lipophilicity and improve solubility while retaining permeability and metabolic stability. Whilst reduced activity of **BZ1** and **BZ1-I** against *Leishmania donovani* (MHOM/SD/62/1S-CL2D, LdBOB) compared to the *L. donovani* (MHOM/IN/80/DD8) intracellular amastigote was observed, both compounds fulfill the DNDi target candidate profile criteria for promising molecules based on this in vitro activity profile in terms of activity and selectivity. As a result, **BZ1** and **BZ1-I** progressed for evaluation in a *L. infantum chagasi* (strain MHOM/BR/1972/BH46) chronic hamster model for visceral leishmaniasis[55,56].

The in vivo model used incorporates GLU (meglumine antimoniate), belonging to the class of antimonials, as the reference drug. Antimonials remain the treatment of choice in South America, Africa, Nepal, Bangladesh, and India (except North Bihar)[21]. GLU at a dose of 50 mg/kg/day via intraperitoneal route reduced the parasite burden to 99.21% and 98.79% in spleen and liver, respectively. The efficacy of GLU corresponds to the values reported previously for the same dosage regimen[56,57]. Both **BZ1** and **BZ1-I** showed excellent in vivo activity when administered orally (10 mg/kg/day), with **BZ1** being comparable to GLU, reducing parasitemia to 98.56% and 98.36% in the spleen and liver, respectively. Of particular note, **BZ1-I** was found to be more active than GLU, with parasite load reduced to 99.95% in spleen and 99.99% in liver. The efficacy of both **BZ1** and **BZ1-I** illustrates that these are highly effective molecules fulfilling the criteria for a lead molecule (DNDi's target product profile) for visceral leishmaniasis[29].

In the experimental visceral leishmaniasis hamster model, the main organs affected are the liver and spleen, where the disease presents a specific organ immune response[58]. In our study, the main histopathological changes observed in the liver were the presence of periportal infiltrate and nodules. The development of granulomas in the liver is closely associated with an attempt from the immune system to control *Leishmania* infection[59]. Furthermore, the main changes observed in the spleen included increased macrophages forming nodular aggregates and granulomas, as well white pulp hypoplasia as previously described by Corbett[60], when animals reach 60 days of infection. The reduction in granulomas observed in both **BZ1** and **BZ1-I** treated groups demonstrated that the compounds were effective at controlling the infection. Mangoud et al. has demonstrated that an increase in the number of granulomas and subsequent formation of necrosis and fibrosis occurs with the progression of infection caused by *L. infantum chagasi*[61], which was observed in the UTG controls.

In the present study, we investigated cellular immune responses by evaluating the mRNA expression of the proinflammatory (TNF-α, IFN-γ and IL-17) and anti-inflammatory (IL-4, IL-10 and TGF-β) cytokines in the spleen and liver samples collected from different groups as previously described[62]. The GLU treated animals were found to have an increased INF-γ (Th1) expression, which signifies a decrease in the parasitic load. The same effect has been seen in miltefosine treated VL-hamsters' models in which the animals exhibit a resistance to infection[63,64]. A similar trend with compound **BZ1** was shown, where it shifted the profiles more towards the healthy controls compared with the untreated control (UTG) showing a decrease in parasitic load. Earlier studies have also indicated that a high expression of IL-10 and TGF-β suggests parasite proliferation and establishment of an active infection[64,65]. In the present study, this was observed in the UTG group compared to the CTL (healthy, uninfected) group. Interestingly, both **BZ1** and **BZ1-I** have decreased expression of TGF-β when compared to UTG in spleen samples. This correlates with the reduction of the granulomas observed with both **BZ1** and **BZ1-I**, and better spleen architecture and

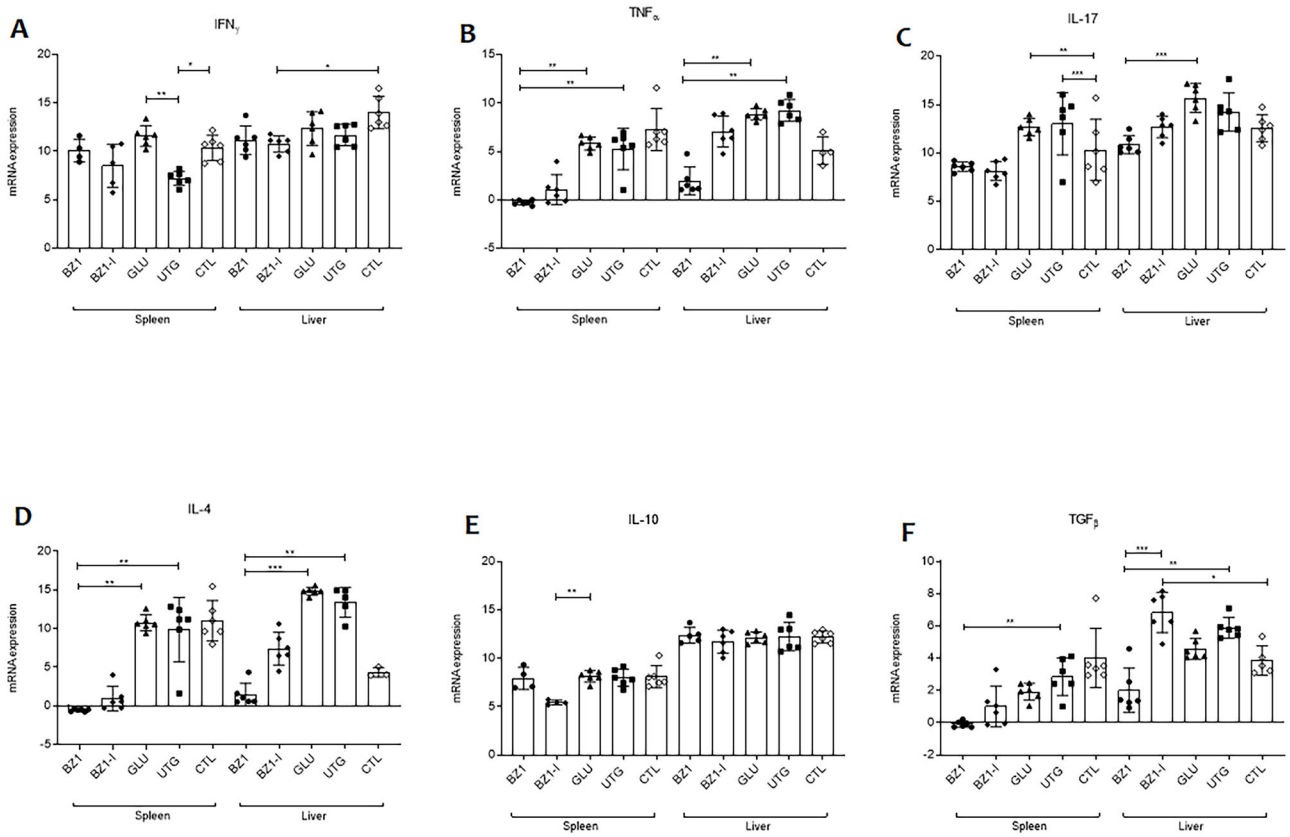

Fig. 10 | Cellular immune response (pro-inflammatory and anti-inflammatory) in liver and spleen cells of healthy (uninfected), untreated (UTG); treated with GLU; or treated with BZ1 or BZ1-I compounds. INF-γ (**A**), TNF-α (**B**), IL-17 (**C**), IL-4 (**D**), IL-10 (**E**), and TGF-β (**F**) with the material obtained from the spleen and liver fragments of the *L. infantum chagasi* (MHOM/BR/1972/BH46) Hamster model. CTL: Healthy (uninfected) animals, GLU: meglumine antimoniate, UTG: untreated control.

preserved periportal spaces of the liver when compared to the untreated controls signifying susceptibility to infection.

Collectively, the in vitro and in vivo data provides strong evidence of selective anti-leishmanial activity and efficacy against both new and old-world strains of *Leishmania*. Current efforts, including whole genome sequencing, are focused on ascertaining the biological target or mode of action to enable more extensive interrogation for new further optimized lead molecules. Focused medicinal chemistry optimization, exploring the structure activity relationships of this chemical class and incorporating more comprehensive pharmacological profiling, is thus warranted.

Conclusion

Here we have discussed the identification and development of lead compounds which fulfill the DND*i* target candidate profile with promising activity, being selective for the parasite with minimal effect on host cells. Of note, these compounds demonstrated activity across multiple species and strains of *Leishmania* parasite representative of both the Old and New World. The data generated to date provides evidence to support further investigation and development of the lead series, with the potential to develop a new anti-leishmanial drug candidate.

Methods

Library specifications, reference compound and assay plate preparation

A subset of 5560 compounds representative of a larger diverse synthetic scaffold library housed within Compounds Australia®, a compound management facility based at Griffith University, Australia, were screened. The scaffold library is comprised of >33,000 pure compounds, acquired from various commercial vendors including Enamine® and ChemDiv®, ~30 compounds per scaffold (1200 scaffolds in total). The 5560 compounds collection was handpicked as a representative set of the total 1200 scaffolds within the library.

For the initial screen, compounds were provided by Compounds Australia® in master plates in single point 5 mM concentrations in 100% DMSO. These compounds were diluted in RPMI without heat inactivated fetal bovine serum (HIFBS) and screened at 10 (for promastigotes) and 20 μM (for intracellular amastigotes) as 0.4% dimethyl sulfoxide (DMSO) for the promastigote and intracellular amastigote assays, respectively. The data was normalized with in-plate controls based on 100% inhibition of parasites with 1 μM amphotericin B, 0% parasite inhibition in the presence of 0.4% DMSO, and the percentage inhibition of each test molecule was calculated for each concentration. Retest of the active hits (with 60% activity in the promastigote assay and 50% activity in the intracellular amastigote assay) was performed using the following concentration range, 20–0.2 μM (0.4% DMSO vehicle) based on a 7-point concentration response scale. New stocks of the active hits were ordered, and their activity was assessed. Amphotericin B, miltefosine and VL-2098[66] were used as reference drugs and compounds.

In vitro anti-leishmanial assays

***L. donovani* DD8 promastigote viability assay**. An initial parasite density of 1×10^5 parasites/mL was inoculated into a 75 cm^2 flask (in a total of 30 mL of M199 medium + 10% (v/v) HIFBS) and incubated at 27 °C. After 96 h, the parasites reached the mid-log phase and were seeded in the 384-well Greiner™ black/clear bottom plates at a concentration of 5×10^5 parasites/mL in a volume of 55 μL using an Agilent BRAVO™ automated liquid handling platform. The stocks were diluted 1:25 in M199 media without HIFBS using a dilution plate. The

compounds were dispensed in 5 µL using an Agilent BRAVO™ and plates incubated for an additional 68 h at 27 °C at normal atmospheric conditions. Resazurin was then added (0.142 mM final assay concentration) to the plates in a volume of 10 µL/well using a Multidrop™ 384 Reagent Dispenser (Thermo Scientific®, Newington, NH) and incubated at 27 °C at normal atmospheric conditions. The plates were read after 4 h using an EnVision™ Multilabel plate reader (PerkinElmer®) using fluorometry settings with excitation of 530 nm and emission 590 nm. The IC_{50} value for each compound was calculated by normalizing the data based on 1 µM amphotericin B (100% inhibition of parasites) serving as the positive control and 0% inhibition = 0.4% DMSO as the negative control against log of concentration in PRISM™ 10 software (GraphPad Software Inc., San Diego, CA) (denoted IC_{50} by PRISM™). Each compound concentration was screened in duplicate.

Leishmania infantum chagasi and Leishmania amazonensis promastigote viability assay. Promastigotes of the species *Leishmania infantum chagasi* (MHOM/BR/72/BH46) were cultured in Schneider's medium, supplemented with 10.0% (v/v) heat-inactivated fetal bovine serum (FBS) and 1.0% penicillin (10,000 UI mL^{-1})/streptomycin (10.0 mg mL^{-1}) (Sigma, USA) and *Leishmania amazonensis* (MHOM/BR/71973/M2269) were grown in LIT medium, supplemented with 10.0% (v/v) HIFBS and 1.0% penicillin (10,000 UI mL^{-1})/streptomycin (10.0 mg mL^{-1}) (Sigma, USA).

Log-phase growth promastigotes were added to 96-well cell culture plates (tissue culture treated) at a concentration of 1×10^6 cells per well with compounds BZ1 and BZ1-I in triplicate (concentration range: 100–0.781 µg/mL dilution 1:2 in DMSO 0.6% v/v). Amphotericin B, 9.24 µg/mL was used as positive control. Cultures were maintained in 5% CO_2 at 25 °C in a 72 h incubation, then washed with PBS and centrifuged three times at 3000 rpm for 10 min at 4 °C for the removal of the compounds. The promastigote viability analysis was performed using 100 µL/well of a sterile solution of a 4 µg/mL 3-(4,5-dimethylthiazol-2-yl)-2,5-diphenyltetrazolium bromide (MTT) in phosphate buffered saline (PBS), incubated for 4 h, followed by the addition of 50 µL DMSO. The reading was undertaken using wavelength 560 nm. Using GraphPad Prism, version 5.0 the dose response curves were generated and the IC_{50} estimated. The second experiment was performed using a compound concentration range from 5 to 0.039 µg/mL.

Murine peritoneal macrophages for cytotoxicity studies were obtained from the peritoneal lavage of Swiss mice, performed in accordance with the Guide for the Care and Use of Laboratory Animals, and approved by the Research Ethics Commission of the Universidade Federal de Alfenas. A suspension of 1×10^6/mL murine peritoneal macrophages, in RPMI 1640 medium, supplemented with 10.0% HIFBS, and 1% penicillin (10,000 UI/mL)/streptomycin (10 mg/mL) was added to each well in 96-well plates. The plates were incubated in a 5% CO_2 air mixture at 37 °C to allow for adhesion of the cells. After 24 h, non-adherent cells were removed by washing with the RPMI 1640 medium. Then, compounds and reference drugs, at concentrations ranging from 500 to 3.9 µg mL^{-1} in DMSO at the final concentration of 0.6% (v/v), were added to the wells containing the cells and the plates incubated for 48 h. Non-adherent cells were removed by washing with the RPMI 1640 medium, and MTT) added to RPMI 1640 medium. The absorbance of each individual well was calculated at 570 nm. Each experiment was performed in triplicate, and the percentage of viable cells was calculated using GraphPad Prism, version 5.0. The second experiment also was performed at concentrations ranging from 5 to 0.039 µg/mL.

***L. donovani* MHOM/IN/80/DD8 intracellular amastigote assay**. The *L. donovani* MHOM/IN/80/DD8 intracellular amastigote assay[54] was used to determine the IC_{50} values of the compounds against *L. donovani* DD8 intracellular amastigotes described briefly as follows:

Cell culture: L. donovani MHOM/IN/80/DD8 (ATCC 50212) promastigote parasites were maintained in modified M199 Hanks salt medium (pH 6.8) supplemented with 10% heat-inactivated fetal bovine serum (FBS) at 27 °C. Parasites were subcultured every 7 days at a concentration of 10^5 cells/mL. THP-1 (ATCC TIB202) cells were maintained in RPMI medium and 10% FBS at 37 °C/5% CO_2. The cells were subcultured every 2–3 days to maintain a cell density between 2×10^5 and 1×10^6 cells/mL.

Assay protocol: THP-1 cells were seeded in 384-well cell carrier imaging plates (PerkinElmer, Waltham, MA) using a Bravo automated liquid handling platform (Agilent Technologies, Santa Clara, CA, USA) at a concentration of 12,500 cells per well in RMPI plus 10% HIFBS medium containing 25 ng of phorbol 12-myristate 13-acetate (PMA)/mL in order to induce differentiation of the THP-1 cells. Assay plates were incubated at room temperature for 30 min to allow cells to adhere before being incubator at 37 °C and 5% CO_2 for 24 h. After incubation, the PMA was removed by discarding the medium within wells and washing the assay plates three times in phosphate-buffered saline (PBS) on an HydroSpeed plate washer (Tecan, Melbourne, VIC, Australia). After washing, 40 µL of fresh RMPI and 10% FBS medium were added to the assay plates, followed by incubation for 48 h at 37 °C and 5% CO_2.

The number of metacyclic promastigotes present in a 7-day-old *L. donovani* DD8 promastigote culture was subsequently determined, and parasites were added to the assay plates containing the transformed THP-1 cells (72 h after initial cell seeding) at a multiplicity of infection of 1:2.5 (ratio of host cells to parasites). Assay plates were incubated at room temperature for 30 min, followed by 24 h incubation at 37 °C and 5% CO_2. Non-internalized parasites were subsequently removed by aspirating the medium within wells and washing the assay plates three times in PBS on a HydroSpeed plate washer before the addition of 45 µL of fresh RMPI (10% FBS and 25 ng/mL PMA). Controls consisted of positive wells containing a final assay concentration of 1 µM amphotericin B, and negative wells containing 0.4% DMSO were used as in-plate controls for all experiments. Then, 1 µL of each compound, prepared by Compounds Australia, was diluted by the addition of 24 µL of RPMI medium containing no FCS. Next, 5-µL portions of this dilution were dispensed via a Bravo liquid handler to assay plates to give final assay concentrations of 80 µM (at 0.4% DMSO). For IC_{50} confirmation, the final assay concentrations ranged from 80 to 0.004 µM. Assay plates were incubated for 96 h at 37 °C and 5% CO_2 before being fixed with 4% paraformaldehyde and stained with SYBR green and CellMask Deep Red (ThermoFisher Scientific, Wlatham, MA, USA).

Images were acquired on an Opera high-content imaging system (Perkin-Elmer). Healthy host (THP-1) cells were identified based on the CellMask Deep Red cytoplasmic and SYBR green nuclear area and intensities. Segmentation of nuclear and cell boundaries were used to identify the region of host cell cytoplasm. Intracellular parasites were then identified within this region based on spot detection algorithms of the SYBR green staining (with size and intensity measurements used to define parasite nucleus of kinetoplast) to determine the number of parasites present within THP-1 host cells. An infected cell was defined as a host cell containing >3 parasites within the cytoplasm boundary. The compound activity was determined based on the number of infected cells normalized to the positive (1 µM Amphotericin B) and negative (0.4% DMSO) controls. Non-linear sigmoidal dose–response curves with no constraints were plotted, and IC_{50} values were calculated using GraphPad Prism 6 from two independent experiments.

***L. donovani* MHOM/SD/62/1S-CL2D, LdBOB intracellular amastigote assay**. The *L. donovani* MHOM/SD/62/1S-CL2D, LdBOB intracellular amastigote assay was performed as previously described[33], with minor modifications. In brief, a 96 h incubation period was utilized to replace the 72 h incubation period with compound treated infected cells. The selectivity of the compounds was assessed using THP-1 host cells.

Determination of the cidal action of compounds. To determine the cidal action of the selected compounds, the promastigotes from two different cultures in two separate M199 media ($N = 2$) were seeded at a concentration of 5×10^5 parasites/mL and volume of 55 µL/well in

Greiner 384-well plates using a Bravo liquid handler. A master compound plate was created with the compounds dissolved in 100% DMSO diluted in M199 + 10% HIFBS media using a dilution plate with the final assay concentration of 66.660, 33.330, 16.660, 6.660, 3.330, 1.660, 0.660, 0.330, 0.160, 0.06, 0.033, 0.016, 0.006 and 0.003 µM. The compound exposure was for 24, 48 and 72 h. The compounds were dispensed from the master plate to the assay plate in a volume of 5 µL into 55 µL of parasite culture/well. Cell numbers were determined using the method described previously[67]. If no cells were identified at the above concentrations, compounds were considered to have been effectively cidal at that time point.

Time to kill assay (promastigote viability assay). To calculate the time to kill for compounds in the promastigote assay the IC_{50} values were determined for compounds **BZ1, BZ1-I** and reference compounds (amphotericin B and miltefosine) following exposure of the promastigotes to compound and reference drugs for 24, 48 and 72 h. The starting concentration was 40 µM and the IC_{50} values were determined from a 14-point concentration–response curve. The compound exposure was for 24, 48, 72 and 96 h.

Time to kill assay (Intracellular amastigote assay). To calculate the time to kill for compounds in the intracellular amastigote assay the IC_{50} values were determined for compounds **BZ1, BZ1-I** and reference drugs (amphotericin B and miltefosine) following incubation for 24, 48 and 72 h. The starting concentration was 40 µM and the IC_{50} values were determined from a 14-point concentration-response curve. The assay conditions were the same as previously described for the intracellular amastigote assay.

Host cell and compound pre-incubation studies. A study was performed to assess the percentage infectivity in the host cells after pre-incubation with **BZ1, BZ1-I** and reference drugs (amphotericin B and miltefosine) at various time points (12, 24, 48 and 72 h). THP-1 cells were plated as described previously[54], after 24 h, cells were washed 3 times with PBS and 45 µL RMPI + 10% HIFBS (v/v) added to the assay plates. The reference compounds and **BZ1** and **BZ1-I** were diluted 1:25 in RPMI with no HIFBS with a final assay concentration in a 14-point concentration response ranging from 80 to 0.004 µM. Five µL were dispensed into assay plates using a Bravo liquid handler (Agilent). The assay plates were incubated for 24, 48 and 72 h at 37 °C/5% CO_2. After 24, 48 and 72 h the plates were washed 3 times with PBS. The addition of parasites, washing the extracellular parasites away and staining the plates were subsequently performed as mentioned previously.

Cytotoxicity assays. The HepG2, RAW-264.7, J774.1 and macrophage (Induced THP-1) resazurin viability assays were undertaken as a modification of the HEK-293 resazurin viability assay previously described[54].

HEK-293 resazurin viability assay. HEK-293 human embryonic kidney cell line obtained from the ATCC®, USA (HEK-293 CRL-1573™) was maintained in DMEM supplemented with 10% (v/v) HIFBS at 37 °C in a humidified atmosphere of 95% air and 5% CO_2. The cells were passaged as they reached 80% confluence. The assay was undertaken as previously described[54].

HepG2 resazurin viability assay. HepG2 cells, a human liver cancer cell line obtained from the ATCC®, USA (Hep G2-ATCC® HB-8065™), were maintained in DMEM supplemented with 10% (v/v) HIFBS at 37 °C in a humidified atmosphere of 95% air and 5% CO_2. HepG2 cells at 5×10^4 cells/mL in DMEM + 10% HIFBS (v/v), were added in a total volume of 55 µL to Greiner™ black 384-well plates using the Multidrop™ liquid handling system. The compounds prepared at 20 mM in 100% DMSO were diluted in DMEM without HIFBS in a ratio 1:25 and 5 µL of the compounds were added to give a final concentration of 0.4% DMSO and desired compound final concentration. The plates were incubated for 48 h at 37 °C with 5% CO_2. Resazurin was diluted in DMEM + 10% HIFBS to give a concentration of 0.49 mM. Ten microliters of this dilution were added to assay plates, which were further incubated for 5 h at 37 °C/5% CO_2, then left at room temperature for 19 h. The plates were read on the EnVision™ Multilabel plate reader using fluorometry settings with an excitation of 530 nm and an emission of 590 nm. DMSO (0.4%) was used as the negative control and 5 µM of puromycin was used as the positive control.

Macrophage (Induced THP-1) cytotoxicity assay. THP-1 cells, a human monocytic cell line obtained from the ATCC®, USA (THP-1 TIB-202™), were maintained in RPMI 1640 medium GlutaMAX™ supplemented with 0.05 mM mercaptoethanol and 10% (v/v) HIFBS at 37 °C in a humidified atmosphere of 95% air and 5% CO_2. The THP-1 cells were suspended at a concentration of 2.5×10^5 cells/mL in RMPI medium + 10% (v/v) HIFBS in a 150 mL sterile clear polystyrene bottle (Corning®). One mg/mL of PMA stock solution was diluted 1:20 in DMSO and then the working solution diluted 1:2000 in cell suspension to give a final concentration of 25 ng/mL. 50 µL of cell suspension at a density of 2.5×10^5 cells/mL were added to Greiner™ black/clear bottomed 384-well plates using a BRAVO™, which was also used for all subsequent additions unless otherwise stated. After 24 h incubation at 37 °C/5% CO_2 the plates were washed 3X with PBS and incubated for an additional 48 h at 37 °C/5% CO_2 in accordance with the intracellular amastigote assay conditions. The reference compounds, amphotericin B, miltefosine were prepared in 100% DMSO, whereas puromycin was prepared in MilliQ water. The reference compounds were serially diluted in 100% DMSO to give 14 concentrations (40 µm–0.002 µM). An intermediate dilution of the reference plate was prepared in water, PBS or RMPI medium and 5 µL of these dilutions subsequently dispensed into the THP-1 assay plates. The plates were incubated for 64 h at 37 °C/5% CO_2. Cell viability was assessed using resazurin at a concentration of 1.5 mM (0.3 mM final assay concentration) in a volume of 10 µL using a Multidrop™ 384 Reagent Dispenser for an incubation period of 8 h. The plates were read on an EnVision™ Multilabel plate reader using fluorometry settings with excitation of 530 nm and emission 590 nm.

RAW-264.7 resazurin viability assay. RAW-264.7 murine macrophage cell line derived from Abelson's leukaemia obtained from the ATCC®, USA (RAW 264.7-ATCC® TIB-71™) was maintained in DMEM supplemented with 10% (v/v) HIFBS at 37 °C in a humidified atmosphere of 95% air and 5% CO_2. The protocol used was as described for the THP-1 cytotoxicity assay with a slight modification in the number of cells initially seeded per 384-well plate: reduced from 2.5×10^5 to 2.0×10^4 cells/mL.

J774.1 resazurin viability assay. J774.1 cell line, a murine macrophage cell line from reticulum cell sarcoma obtained from the ATCC®, USA (J774A.1-ATCC® TIB-67™), was maintained in DMEM supplemented with 10% (v/v) HIFBS at 37 °C in a humidified atmosphere of 95% air and 5% CO_2. The protocol used was similar to THP-1 cytotoxicity assay with a slight modification in the number of cells initially seeded per 384-well plate: from 2.5×10^5 to 4×10^4 cells/mL.

Statistics and reproducibility. To accurately assess the activity of compounds in inhibiting *Leishmania* parasite survival, the data was normalized based on the number of infected cells in comparison to control samples. The negative control, which contains 0.4% DMSO, represents the baseline or no-compound condition, while reference compound (amphotericin B) serves as positive controls for known activity. By normalizing the data in this manner, the calculated activity of each compound was directly comparable, ensuring a reliable evaluation of their anti-parasitic effects.

The normalization formula used is as follows:

$$\text{Normalization} = 100 - [100 \times (\text{sample} - \text{average of minimum signal}) / (\text{average of maximum signal} - \text{average of minimum signal})]$$

The *Z*-factor, a key statistical parameter used to assess the quality of an assay was calculated for all assays. The *Z*-factor was calculated as follows:

$$Z' = 1 - [3 \times (\text{SD of wells with negative control}) + 3 \times (\text{SD of wells with positive control})] / [\text{Mean of negative control} - \text{Mean of positive control}]$$

A *Z*-factor value close to 1 indicates excellent assay quality, whilst between 0.5 and 1 is typically considered acceptable for cell-based assays.

Drug metabolism and pharmacokinetics studies

Physicochemical parameters using ChemAxon JChem software. A range of physicochemical properties evaluating drug-likeness and likely oral absorption characteristics were calculated using the ChemAxon chemistry cartridge via JChem for Excel software (version 16.4.11). A brief description of each parameter is provided below, along with a suggested ideal range based on research reported in the Absorption, distribution, metabolism, and excretion (ADME) literature from key industry and academic sources.

MW (<500): Molecular weight.

PSApH 7.4 (<140 Å^2): Polar surface area also inversely correlates with membrane permeability.

HBD (<5) and HBA (<10): Number of hydrogen bond donors and acceptors gives an indication of the hydrogen bonding capacity, which is inversely related to membrane permeability.

FRB (≤10): Number of freely rotating bonds represents the flexibility of a molecule's conformation.

Aromatic rings (<4): Total number of aromatic and heteroaromatic rings is also related to molecular flexibility.

Fsp^3 (>0.3): Fraction of sp^3 carbons to total carbons indicates the complexity of a molecule's 3D structure.

cpK_a: Ionization constants impact solubility and permeability. Only physiologically relevant predicted values are provided here (i.e. $0 < pK_a < 12$).

cLogP/cLogDpH (<5): Partition coefficients reflect the lipophilic character of the neutral structure, while distribution coefficients reflect the partitioning properties of the ionized molecule at a specific pH.

Kinetic solubility estimation using nephelometry (SolpH). Compound in DMSO was spiked into either pH 6.5 phosphate buffer or 0.01 M HCl (pH ~2.0) with the final DMSO concentration being 1%. After 30 min had elapsed, samples were then analyzed via Nephelometry to determine a solubility range. See Bevan and Lloyd (2000) Anal Chem, 72:1781-1787.

Distribution coefficient estimation using chromatography (gLogDpH). Partition coefficient values (Log*D*) of the test compounds were estimated at pH 7.4 by correlation of their chromatographic retention properties against the characteristics of a series of standard compounds with known partition coefficient values. The method employed is a gradient HPLC based derivation of the method developed by Lombardo (see Lombardo et al. (2001) J. Med. Chem. 44:2490–2497).

In vitro metabolic stability

Incubation. The metabolic stability assay was performed by incubating each test compound in liver microsomes at 37 °C and a protein concentration of 0.4 mg/mL. The metabolic reaction was initiated by the addition of an NADPH-regenerating system and quenched at various time points over a 60-min incubation period by the addition of acetonitrile containing diazepam as internal standard. Control samples (containing no NADPH) were included (and quenched at 2, 30 and 60 min) to monitor for potential degradation in the absence of cofactor. The human liver microsomes used in this experiment were supplied by XenoTech, lot #1410230. Microsomal incubations were performed at a substrate concentration of 0.5 µM.

Data analysis. Species scaling factors from Ring et al.[68] were used to convert the in vitro Clint (µL/min/mg) to an in vivo CLint (mL/min/kg). Hepatic blood clearance and the corresponding hepatic extraction ratio (EH) were calculated using the well stirred model of hepatic extraction in each species, according to the "in vitro T1/2" approach[69]. The EH was used to classify compounds as low (<0.3), intermediate (0.3–0.7), high (0.7–0.95) or very high (>0.95) extraction compounds. Predicted in vivo clearance values have not been corrected for microsomal or plasma protein binding. Species scaling calculations are based on two assumptions: (1) NADPH-dependent oxidative metabolism predominates over other metabolic routes (i.e. direct conjugative metabolism, reduction, hydrolysis, etc.) and (2) rates of metabolism and enzyme activities in vitro are truly reflective of those that exist in vivo. If significant non-NADPH-mediated degradation is observed in microsome control samples, then assumption (1) is invalid and predicted clearance parameters are therefore not reported.

In vivo anti-leishmanial assay

Ethics statement. All experimental procedures involving animals were approved by the Research Ethics Commission of the Federal University of Alfenas, Brazil (project number 394/2012), and were performed according to the Guide for the Care and Use of Laboratory Animals[70]. We have complied with all relevant ethical regulations for animal use.

Experimental animals. Male golden hamsters (*Mesocricetus auratus*) recently weaned (~120 g) were housed inside boxes with sterile absorbent material, with food and water ad libitum, on ventilated shelves with controlled local temperature and in natural light/dark cycle. Hamsters were infected intraperitoneally with 1×10^7 promastigotes of *L. (L.) infantum chagasi* (MHOM/BR/1972/BH46) and maintained in sterile absorbent material boxes, with water and food ad libitum.

In vivo model for Leishmaniasis. The *L. chagasi* in vivo evaluation was performed as previously described by Colombo et al.[57]. During the chronic phase of infection (~60 days post infection), animals were divided into 4 groups, and subjected, to one of the following treatments for 10 consecutive days; vehicle 0.5% of carboxymethyl cellulose (vehicle) suspension ($n = 5$ animals), administered orally (untreated group, or UTG); 50 mg/kg/day of GLU, by intraperitoneal injection (GLU group; $n = 5$); 10 mg/kg/day of compounds **BZ1** and **BZ1-I**, administered orally as suspensions in 0.5% of carboxymethyl cellulose ($n = 6$ each group). After 10 days of treatment, animals were sacrificed in a CO_2 chamber, and a sample of the spleen and the liver (~50 mg) removed, weighed and used for total RNA extraction.

DNA extraction for standard curve. Standard curves of parasite DNA for use in quantitative real-time PCR (qPCR) experiments were produced as described previously[71]. Briefly, promastigotes from stationary phase cultures were harvested by centrifugation at 1000×*g* for 10 min, washed twice in PBS (pH 7.2), and counted in a hemocytometer. Then, parasites were re-suspended in PBS (pH 7.2) to a concentration of 1×10^8 cells/mL, and serially diluted (1:10) up to a concentration of 1×10^2 cells/mL (in triplicates). Lysis buffer (10 mM Tris–HCl, pH 8.0, containing 10 mM EDTA, 0.5% SDS, 0.01% N-Lauroylsarcosine sodium salt, 100 µg/mL Proteinase K) was then added to parasite suspensions, at a ratio of 1:4 (v/v), samples were mixed by vortexing and incubated at 56 °C, for 40 min. DNA was extracted from lysed samples using the QIAamp DNA extraction Mini Kit (Qiagen), according to the manufacturer's instructions.

RNA extraction and cDNA synthesis. Fragments of liver and spleen (~50 mg; weighed using sterile and disposable surgical material) removed from treated mice were placed in sterile microfuge tubes and frozen immediately at −80 °C in storage buffer (RNAlater, Thermofisher). RNA extraction was performed 24 h after fragment removal, using the RNeasy Mini Kit (Qiagen), according to the manufacturer's instructions. RNA samples were frozen immediately after extraction. For reverse-transcription into cDNA, 1 µl of dNTPs mix (10 mM) and 1 µl of random primers (3 µg/µL) were added to 11 µl of RNA sample, and samples were incubated in a thermal cycler for ~5 min, at 65 °C. Then, tubes were placed on ice for 20 s, and 2 µl of DTT (100 mM) and 4 µl 5x buffer (Tris–HCl 250 mM, pH 8.3, containing 375 mM KCl, 15 mM $MgCl_2$) were added, and samples incubated again in the thermal cycler for 20 s, at 37 °C. Finally, 1 µl (200 U/µL) M-MLV RT enzyme was added and samples incubated for 50 min, for cDNA synthesis. The purity of the cDNA sample was confirmed by measuring the absorbance at 260/280 in a NanoDrop ND2000, and sample integrity was verified by agarose gel electrophoresis and PCR. Samples were frozen at −20 °C for subsequent use in qPCR[57].

Parasite load estimation by LINJ31 quantitative PCR (qPCR). Quantitative real time PCR (qPCR) was performed using the TaqMan® probe 5'CCT CCT TGG ACT TTG C3' (double-labeled with FAM at the 5'-end and a non-fluorescent quencher at the 3'-end), and the primers LINJ31F (5'CCG CGT GCC TGT CG3') and LINJ31R (5'CCC ACA CAA GGA GCG ACT3'), which amplify *L. (L.) infantum* hypothetical protein (partial mRNA; GeneBank accession number LinJ31.1310). Reactions were performed in a StepOne Real Time PCR System (Applied Biosystems), and reaction mixtures contained 2 µL of DNA or cDNA samples, 10 µL of 2X TaqMan Universal PCR Master Mix, 1 µL of a mixture of forward (LINJ31F) and reverse (LINJ31R) primers (at a concentration of 18 µM), and 5 µM of the labeled TaqMan® probe, in a final volume of 20 µL. For negative and positive controls, water or DNA extract from *L. (L.) infantum chagasi* (MHOM/BR/1972/BH46 were added, respectively. The following PCR conditions were used: one step of 50 °C for 2 min, followed by one step of 95 °C for 10 min, and 40 cycles of 95 °C for 15 s and 60 °C for 1 min. The number of parasites per gram of spleen or liver tissue was calculated based on the linear regression data from the standard curve performed with promastigote DNA. Statistical analysis was performed by quantitative Student's *t*-test with Mann–Whitney (unpaired, two-tailed) for the significance test ($p < 0.05$)[72].

Histopathological assays. The *L. chagasi* histopathological assay was performed as previously described by Silva et al.[62]. Male golden hamsters (*Mesocricetus auratus*) were housed; infected and treated as described above.

Fragments of spleen and liver were collected, processed histologically, and stained with Haematoxylin and Eosin (HE). The histopathological analyses for the different experimental groups were performed blinded. The spleen slides were analyzed to evaluate the white pulp and red pulp ratio, using Image-Pro Plus software to measure the areas relative to these pulps. The liver slides were analyzed to measure the intensity of the periportal infiltrate and to count of the number of granulomas. Analysis of the liver involved identifying the presence of inflammatory infiltrates, nodules and inflammatory cells (mononuclear and polymorphonuclear cells) in the periportal region. In hepatic parenchyma, the presence of lobular infiltrate, nodules, Kupffer cells hyperplasia and hypertrophy, necrosis and inflammatory cells (mononuclear and polymorphonuclear cells). The inflammatory infiltrate near periportal region and parenchyma were quantified according to intensity (mild, moderate or intense). In the spleen, the presence of hyperplasia or hypoplasia in white pulp were evaluated, in addition to the presence of nodules and inflammatory cells (macrophages, plasmocytes, neutrophils) in red pulp.

Evaluation of the relative expression of cytokines by qPCR. The relative expression of cytokines was measured as previously described by Silva et al.[62]. The assay to evaluate the gene expression of the cytokines IL-10, IL-4, TGFβ, IFN-γ, IL-17 and TNFα was performed with the material obtained from the spleen and liver fragments of the animals. RNA was extracted from the fragments and cDNA synthesized using real-time PCR. The Taqman-type hydrolysis probes used to quantify the relative expression of the cytokines were normalized against hamster microgobulin obtained from the Genebank gene sequence.

The primers were designed using Software Primer Blast and recently published[62]. The nucleotide sequences for the genes evaluated in this study were obtained from GenBank (https://www.ncbi.nlm.nih.gov/genbank/). The primers that were produced by Integrated DNA Technologies (IDT) and their sequences are shown in Table 2.

Primers sequences

IL-10 Primer 1: CCA GCT GGA CAA CAT ACT ACT C
Primer 2: CTG GAT CAT TTC TGA TAA GGT TTG G
Probe: /56-FAM/TG CAG GAC T/Zen/T TAA GGG TTA CTT GGG T/3IABkFQ/
IL-4 Primer 1: GAA GAA CTC CAC GGA GAA AGAC Primer 2: GGG TCA CCT CAT GTT GGA AAT A Probe:/56-FAM/CT TCC CAG G/Zen/T GCT TCG CAA GTT T/3IABkFQ
TGF-β Primer 1: GGC AGC TGT ACA TCG ACT TT Primer 2: GAC AGA AGT TGG CGT GGT AG Probe: /56-FAM/TG GAA GTG G/Zen/A TTC ACG AGC CCA AG/3IABkFQ/
IFN-γ Primer 1: GAG GAG CAT AGA CAC CAT CAA G Primer 2: CCT GAA GGT CAT TTA CCG GAA T Probe: /56-FAM/TC TTC AAC A/Zen/G CAG CAT GGA GAA ACT CA/3IABkFQ/
IL-17 Primer 1: CTC CAG CAG CAA CTC TTC TT Primer 2: TCT TCT GTT GCT GGT CTC TTG Probe: /56-FAM/CC AGC CAG G/Zen/G TTC TTC TCA AGC TC/3IABkFQ/
TNF-α Primer 1: GGT TTA CTC CCA GGT TCT CTT C Primer 2: GGA CAG GAG GTT GAC GTT AT Probe: /56-FAM/TC AGC CGC A/Zen/T TGC TGT GTC CTA /3IABkFQ/
MG (Microglobulin, hamster constitutive gene) Primer 1: GGT CTT TCT ATC TCT TGG CTC A Primer 2: CTT GGG CTC CTT CAG AGT TAT G Probe: /HEX/ACT GCG ACT/ Zen/ G ATA AAT ACG CCT GCA/3IABkFQ/

The reactions were carried out in a Step One Real Time PCR System (Applied Biosystems), in a final volume of 10 µL per reaction. 0.5 µL of a mixture including the forward, reverse, and the TaqMan probe, labeled with Fluorescein amidites (FAM) for the cytokines and Hexachloro-fluoresceine (HEX) for the constituent gene, were added using non-fluorescent quencher (NFQ) on the plate. Then a mix containing 5 µL of 2X TaqMan Universal PCR Master Mix and 3.5 µL of DNAse and RNAse free water and 1 µL of cDNA from the samples were prepared. Homogenization was performed

for all markers, to standardize with the same final concentration of cDNA, and then added to the plate. A negative control of DNAse and RNAse free water was used for each marker. Amplifications occurred with an initial cycle of 50 °C for 2 min; then a cycle at 95 °C for 10 min followed by 40 cycles at 95 °C for 15 s and a final 60 °C step for 1 min. The results were expressed by the ΔCt (Cycle Threshold) method, which consists of a relative quantification, where normalization of expression of each target is performed by subtracting the Ct value found for each cytokine, by the Ct value of the constitutive gene.

Selection of resistant parasites

Amphotericin B, miltefosine and compounds **BZ1** and **BZ1-I** were used to select resistant parasites to assess any differences in THP-1 cell infectivity and determine whether resistance could be maintained in the intracellular amastigote assay. The promastigotes were cultured in the presence of gradually increasing concentrations of amphotericin B, miltefosine, and either compound **BZ1** or **BZ1-I** beginning at starting concentrations of 0.000135 µM (0.125 µg/mL), 0.03330 µM (13.572 µg/mL), 0.0033 µM (1.004 µg/mL) and 0.0033 µM (1.004 µg/mL) respectively, (a sublethal concentration) to generate drug-resistant strains. Throughout the process the concentrations for amphotericin B, miltefosine, **BZ1** and **BZ1-I** were increased gradually and only once the cells displayed growth and mobility characteristics after 96 h incubation comparable to the control cultures grown in the absence of compounds.

Three independent experiments were performed (the promastigotes from three different cultures in three separate M199 media were seeded in 25 cm^2 flasks at a concentration of 5×10^5 promastigotes/mL in a volume of 10 mL) with amphotericin B, miltefosine, compounds **BZ1** and **BZ1-I** at sublethal concentrations. These cultures were sub-cultured every 96 h with the addition of amphotericin B, miltefosine, compounds **BZ1** and **BZ1-I**.

Confirmation of resistant cell lines

For confirming resistance, clonal populations from the resistant parasites were obtained via limiting dilution in a 384-well plate and the confirmation of resistant studies performed on isolated clones.

Resistant clones were evaluated using a promastigote viability assay as described previously. Following confirmation that resistance in the promastigotes was achieved, these cultures were used to infect the THP-1 cells and the infectivity of the cells was assessed. Resistance to amphotericin B, miltefosine, compound **BZ1** and **BZ1-I** was also assessed with the intracellular amastigote assay.

Stability of compound resistance assessed

Following generation of resistant cultures, the sensitivity to the reference drugs (amphotericin B and miltefosine), plus test compounds **BZ1** and **BZ1-I**, were evaluated. In addition, the stability of drug resistance post drug pressure removal throughout time in culture, was assessed. The resistant parasite cultures were grown in the absence of amphotericin B, miltefosine, compounds **BZ1** and **BZ1-I** for 10 passages before the sensitivities of the cultures to these compounds and drugs were retested in the promastigote viability assay and intracellular amastigote assays. This experiment provided an indication as to whether the generated resistance was reversible or not.

Reporting summary

Further information on research design is available in the Nature Portfolio Reporting Summary linked to this article.

Data availability

The authors declare that the data supporting the conclusions of this article are included in the main text and the supplementary materials. The source data underlying the plots in the figures are provided in the Supplementary Data 1 (Excel file).

Received: 23 September 2024; Accepted: 13 June 2025;
Published online: 08 July 2025

References

1. Akhoundi, M. et al. A historical overview of the classification, evolution, and dispersion of Leishmania parasites and sandflies. *PLoS Negl. Trop. Dis.* **10**, e0004349 (2016).
2. DNDi. *Drug for Neglected Diseases Initiative, leishmaniasis Fact Sheet*. https://www.dndi.org/wp-content/uploads/2018/12/DNDi_Leishmaniasis_2018.pdf (2018).
3. Laranjeira-Silva, M. F., Hamza, I. & Perez-Victoria, J. M. Iron and heme metabolism at the Leishmania–host interface. *Trends Parasitol.* **36**, 279–289 (2020).
4. Stockdale, L. & Newton, R. A review of preventative methods against human leishmaniasis infection. *PLoS Negl. Trop. Dis.* **7**, e2278 (2013).
5. Handman, E. Cell biology of Leishmania. *Adv. Parasitol.* **44**, 1–39 (1999).
6. Hendrickx, S., Caljon, G. & Maes, L. Need for sustainable approaches in antileishmanial drug discovery. *Parasitol. Res.* **118**, 2743–2752 (2019).
7. Brindha, J., Balamurali, M. M. & Chanda, K. An overview on the therapeutics of neglected infectious diseases—leishmaniasis and chagas diseases. *Front. Chem.* **9**, 622286 (2021).
8. Roquero, I. et al. Novel chemical starting points for drug discovery in leishmaniasis and chagas disease. *Int. J. Parasitol. Drugs Drug Resist.***10**, 58–68 (2019).
9. Zulfiqar, B. et al. Screening a natural product-based library against kinetoplastid parasites. *Molecules (Basel, Switzerland)* **22**, https://doi.org/10.3390/molecules22101715 (2017).
10. Nagle, A. S. et al. Recent developments in drug discovery for leishmaniasis and human African trypanosomiasis. *Chem. Rev.* **114**, 11305–11347 (2014).
11. Jain, V. & Sharma, A. Repurposing of potent drug candidates for multiparasite targeting. *Trends Parasitol.* **33**, 158–161 (2017).
12. Olías-Molero, A. I., de la Fuente, C., Cuquerella, M., Torrado, J. J. & Alunda, J. M. Antileishmanial drug discovery and development: time to reset the model?. *Microorganisms* **9**, 2500 (2021).
13. Stuart, K. et al. Kinetoplastids: related protozoan pathogens, different diseases. *J. Clin. Investig.* **118**, 1301–1310 (2008).
14. Rama, M., Kumar, N. V. A. & Balaji, S. A comprehensive review of patented antileishmanial agents. *Pharm. Pat. Anal.* **4**, 37–56 (2015).
15. Kamboj, A. K. Leishmaniasis: a public health issue. *J. Altern. Med. Res.* **8**, 297 (2016).
16. Zulfiqar, B. & Avery, V. M. Assay development in leishmaniasis drug discovery: a comprehensive review. *Expert Opin. Drug Discov.* **17**, 151–166 (2022).
17. Nelson, D., La Fon, S. & Tuttle, J. Al-lopurinol ribonucleoside as an antileishmanial agent. *Biol. Chem. J.* **254**, 11544–11549 (1979).
18. Avila, J. & Casanova, M. Comparative effects of 4-aminopyrazolopyrimidine, its 2'-deoxyriboside derivative, and allopurinol on in vitro growth of American Leishmania species. *Antimicrob. Agents Chemother.* **22**, 380–385 (1982).
19. Neal, R. A., Allen, S., McCoy, N., Olliaro, P. & Croft, S. L. The sensitivity of Leishmania species to aminosidine. *J. Antimicrob. Chemother.* **35**, 577–584 (1995).
20. Rangel, H., Dagger, F., Hernandez, A., Liendo, A. & Urbina, J. A. Naturally azole-resistant *Leishmania braziliensis* promastigotes are rendered susceptible in the presence of terbinafine: comparative study with azole-susceptible *Leishmania mexicana* promastigotes. *Antimicrob. Agents Chemother.* **40**, 2785–2791 (1996).
21. Haldar, A. K., Sen, P. & Roy, S. Use of antimony in the treatment of leishmaniasis: current status and future directions. *Mol. Biol. Int.* **2011**, 571242 (2011).
22. Croft, S. L., Sundar, S. & Fairlamb, A. H. Drug resistance in leishmaniasis. *Clin. Microbiol. Rev.* **19**, 111–126 (2006).
23. Croft, S. & Olliaro, P. Leishmaniasis chemotherapy—challenges and opportunities. *Clin. Microbiol. Infect.* **17**, 1478–1483 (2011).

24. Hasnain, M. G. et al. Amphotericin B deoxycholate for relapse visceral leishmaniasis in Bangladesh: a cross-sectional study. *BMC Res. Notes* **11**, 918 (2018).
25. Sundar, S. & Rai, M. Treatment of visceral leishmaniasis. *Expert Opin. Pharmacother.* **6**, 2821–2829 (2005).
26. Escobar, P., Matu, S., Marques, C. & Croft, S. L. Sensitivities of *Leishmania* species to hexadecylphosphocholine (miltefosine), ET-18-OCH(3) (edelfosine) and amphotericin B. *Acta Trop.* **81**, 151–157 (2002).
27. Croft, S. L., Seifert, K. & Yardley, V. Current scenario of drug development for leishmaniasis. *Indian J. Med. Res.* **123**, 399–410 (2006).
28. Sinha, P. K. et al. Phase 4 pharmacovigilance trial of paromomycin injection for the treatment of visceral leishmaniasis in India. *J. Trop. Med.* **2011**, 645203 (2011).
29. Don, R. & Ioset, J. R. Screening strategies to identify new chemical diversity for drug development to treat kinetoplastid infections. *Parasitology* **141**, 140–146 (2014).
30. Zulfiqar, B., Shelper, T. B. & Avery, V. M. Leishmaniasis drug discovery: recent progress and challenges in assay development. *Drug Discov. today* **22**, 1516–1531 (2017).
31. Kar, K., Mukerji, K., Naskar, K., Bhattacharya, A. & Ghosh, D. K. Leishmania donovani: a chemically defined medium suitable for cultivation and cloning of promastigotes and transformation of amastigotes to promastigotes. *J. Protozool.* **37**, 277–279 (1990).
32. Peruhype-Magalhães, V. et al. Immune response in human visceral leishmaniasis: analysis of the correlation between innate immunity cytokine profile and disease outcome. *Scand. J. Immunol.* **62**, 487–495 (2005).
33. De Rycker, M. et al. Comparison of a high-throughput high-content intracellular *Leishmania donovani* assay with an axenic amastigote assay. *Antimicrob. Agents Chemother.* **57**, 2913–2922 (2013).
34. Manna, M. & Khanra, S. Molecular identification of an old clinical isolate of Indian Kala-azar. *J. Parasit. Dis.* **41**, 336–344 (2017).
35. Goyard, S. et al. An in vitro system for developmental and genetic studies of Leishmania donovani phosphoglycans. *Mol. Biochem. Parasitol.* **130**, 31–42 (2003).
36. Pérez-Victoria, F. J. et al. Mechanisms of experimental resistance of Leishmania to miltefosine: implications for clinical use. *Drug Resist. Updat.***9**, 26–39 (2006).
37. Mbongo, N., Loiseau, P. M., Billion, M. A. & Robert-Gero, M. Mechanism of amphotericin B resistance in *Leishmania donovani* promastigotes. *Antimicrob. Agents Chemother.* **42**, 352–357 (1998).
38. Moreira, V. R. et al. Meglumine antimoniate (glucantime) causes oxidative stress-derived DNA damage in BALB/c mice infected by Leishmania (Leishmania) infantum</span&gt. *Antimicrob. Agents Chemother.* **61**, e02360–02316 (2017).
39. Alborzi, A. et al. Effectiveness of short-course meglumine antimoniate (Glucantime®) for treatment of visceral leishmaniasis: a 13-year, multistage, non-inferiority study in Iran. *Am. J. Trop. Med. Hyg.* **96**, 182–189 (2017).
40. Gopu, B., Kour, P., Pandian, R. & Singh, K. Insights into the drug screening approaches in leishmaniasis. *Int. Immunopharmacol.* **114**, 109591 (2023).
41. Ferreira, L. L., de Moraes, J. & Andricopulo, A. D. Approaches to advance drug discovery for neglected tropical diseases. *Drug Discov. Today* **27**, 2278–2287 (2022).
42. Mowbray, C. E. Anti-leishmanial drug discovery: past, present and future perspectives. *Drug Discov. Leishmaniasis* **60**, 24 (2017).
43. Burza, S., Croft, S. L. & Boelaert, M. Leishmaniasis. *Lancet***392**, 951–970 (2018).
44. Sundar, S., Chakravarty, J., Agarwal, D., Rai, M. & Murray, H. W. Single-dose liposomal amphotericin B for visceral leishmaniasis in India. *N. Engl. J. Med.* **362**, 504–512 (2010).
45. Adler-Moore, J. P., Gangneux, J.-P. & Pappas, P. G. Comparison between liposomal formulations of amphotericin B. *Sabouraudia* **54**, 223–231 (2016).
46. Altamura, F., Rajesh, R., Catta-Preta, C. M. C., Moretti, N. S. & Cestari, I. The current drug discovery landscape for trypanosomiasis and leishmaniasis: challenges and strategies to identify drug targets. *Drug Dev. Res.* **83**, 225–252 (2022).
47. Sundar, S. & Chakravarty, J. An update on pharmacotherapy for leishmaniasis. *Expert Opin. Pharmacother.* **16**, 237–252 (2015).
48. Dietze, R. et al. Phase 2 trial of WR6026, an orally administered 8-aminoquinoline, in the treatment of visceral leishmaniasis caused by *Leishmania chagasi*. *Am. J. Trop. Med. Hyg.* **65**, 685–689 (2001).
49. Loiseau, P. M., Cojean, S. & Schrevel, J. Sitamaquine as a putative antileishmanial drug candidate: from the mechanism of action to the risk of drug resistance. *Parasite***18**, 115–119 (2011).
50. Di Giorgio, C., Shimi, K., Boyer, G., Delmas, F. & Galy, J. P. Synthesis and antileishmanial activity of 6-mono-substituted and 3,6-di-substituted acridines obtained by acylation of proflavine. *Eur. J. Med. Chem.* **42**, 1277–1284 (2007).
51. Kevric, I., Cappel, M. A. & Keeling, J. H. New world and old world Leishmania infections: a practical review. *Dermatol. Clin.* **33**, 579–593 (2015).
52. Croft, S. L. & Coombs, G. H. Leishmaniasis—current chemotherapy and recent advances in the search for novel drugs. *Trends Parasitol.* **19**, 502–508 (2003).
53. Altamura, F., Rajesh, R., Catta-Preta, C. M., Moretti, N. S. & Cestari, I. The current drug discovery landscape for trypanosomiasis and leishmaniasis: challenges and strategies to identify drug targets. *Drug Dev. Res.* **83**, 225–252 (2022).
54. Duffy, S. et al. Screening the medicines for malaria venture pathogen box across multiple pathogens reclassifies starting points for open-source drug discovery. *Antimicrob. Agents Chemother.* **61**, https://doi.org/10.1128/aac.00379-17 (2017).
55. Espuri, P. F. et al. Synthesis and evaluation of the antileishmanial activity of silver compounds containing imidazolidine-2-thione. *J. Biol. Inorg. Chem.* **24**, 419–432 (2019).
56. Reimao, J. Q., Colombo, F. A., Pereira-Chioccola, V. L. & Tempone, A. G. Effectiveness of liposomal buparvaquone in an experimental hamster model of *Leishmania* (*L.*) *infantum* chagasi. *Exp. Parasitol.* **130**, 195–199 (2012).
57. Colombo, F., Reis, R., Nunes, J., Dias, D. & Dos Santos, M. In vivo evaluation of leishmanicidal activity of benzophenone derivatives by qPCR. *Med Chem.***7**, 890–893 (2017).
58. Laurenti, M., Sotto, M. N., Corbett, C., Da Matta, V. & Duarte, M. Experimental visceral leishmaniasis: sequential events of granuloma formation at subcutaneous inoculation site. *Int. J. Exp. Pathol.* **71**, 791 (1990).
59. Vianna, V., Takiya, C. & de Brito-Gitirana, L. Histopathologic analysis of hamster hepatocytes submitted to experimental infection with *Leishmania donovani*. *Parasitol. Res.* **88**, 829–836 (2002).
60. Corbett, C., Paes, R., Laurenti, M., Júnior, H. A. & Duarte, M. Histopathology of lymphoid organs in experimental leishmaniasis. *Int. J. Exp. Pathol.* **73**, 417 (1992).
61. Mangoud, A., Ramadan, M., Morsy, T., Amin, A. & Mostafa, S. Histopathological studies of Syrian golden hamsters experimentally infected with *Leishmania D. infantum*. *J. Egypt. Soc. Parasitol.* **27**, 689–702 (1997).
62. da Silva, J. C. et al. Leishmanicidal activity in vivo of a miltefosine derivative in *Mesocricetus auratus*. *Acta Trop.* **209**, 105539 (2020).
63. Trinchieri, G. Interleukin-10 production by effector T cells: Th1 cells show self control. *J. Exp. Med.* **204**, 239–243 (2007).

64. Gupta, R. et al. Treatment of Leishmania donovani-infected hamsters with miltefosine: analysis of cytokine mRNA expression by real-time PCR, lymphoproliferation, nitrite production and antibody responses. *J. Antimicrob. Chemother.* **67**, 440–443 (2012).
65. Corrêa, A. P. F. L., Dossi, A. C. S., de Oliveira Vasconcelos, R., Munari, D. P. & de Lima, V. M. F. Evaluation of transformation growth factor β1, interleukin-10, and interferon-γ in male symptomatic and asymptomatic dogs naturally infected by *Leishmania (Leishmania) chagasi*. *Vet. Parasitol.* **143**, 267–274 (2007).
66. Gupta, S. et al. Nitroimidazo-oxazole compound DNDI-VL-2098: an orally effective preclinical drug candidate for the treatment of visceral leishmaniasis. *J. Antimicrob. Chemother.* **70**, 518–527 (2015).
67. Sykes, M. L. et al. Identification of compounds with anti-proliferative activity against *Trypanosoma brucei brucei* strain 427 by a whole cell viability based HTS campaign. *PLoS Negl. Trop. Dis.* **6**, e1896 (2012).
68. Ring, B. J. et al. PhRMA CPCDC initiative on predictive models of human pharmacokinetics, part 3: comparative assessement of prediction methods of human clearance. *J. Pharm. Sci.* **100**, 4090–4110 (2011).
69. Obach, R. S. Prediction of human clearance of twenty-nine drugs from hepatic microsomal intrinsic clearance data: an examination of in vitro half-life approach and nonspecific binding to microsomes. *Drug Metab. Dispos.* **27**, 1350–1359 (1999).
70. National Research Council. *Guide for the Care and Use of Laboratory Animals* 8th edn (National Academies Press, 2011).
71. Colombo, F. A. et al. Performance of a real time PCR for leishmaniasis diagnosis using a *L. (L.) infantum* hypothetical protein as target in canine samples. *Exp. Parasitol.* **157**, 156–162 (2015).
72. Colombo, F. A. et al. Detection of *Leishmania (Leishmania) infantum* RNA in fleas and ticks collected from naturally infected dogs. *Parasitol. Res.* **109**, 267–274 (2011).

Author contributions

B.Z. performed and analysed data for the in vitro experiments and resistant studies of *Leishmania donovani* (MHOM/IN/80/DD8). F.A.C., J.B.N., P.F.S., and M.J.M. performed and analysed data for the in vivo assays of *Leishmania infantum chagasi* (MHOM/BR/1972/BH46) and cytokine assays. S.M. and M.D.R. performed and analysed data for the in vitro experiments of *Leishmania donovani* (MHOM/SD/62/1S-CL2D, LdBOB). A.F.F. performed and analysed the histopathological data. B.Z. generated all figures. B.Z. and V.M.A. conceived and designed the project. B.Z. and V.M.A. drafted the manuscript. V.M.A. supervised the project and critical revision of the manuscript. All authors have read and approved the final version of the manuscript.

Competing interests

The authors declare no competing interests.

Additional information

Supplementary information The online version contains supplementary material available at https://doi.org/10.1038/s42003-025-08386-0.

Correspondence and requests for materials should be addressed to Vicky M. Avery.

Peer review information *Communications Biology* thanks David D. N'Da and the other, anonymous, reviewers for their contribution to the peer review of this work. Primary Handling Editors: Nishith Gupta and Johannes Stortz. A peer review file is available.